CLOSING IN ON A SHORT-HARD BURST PROGENITOR: CONSTRAINTS FROM EARLY-TIME OPTICAL IMAGING AND SPECTROSCOPY OF A POSSIBLE HOST GALAXY OF GRB 050509b

J. S. Bloom,[1] J. X. Prochaska,[2] D. Pooley,[1,3] C. H. Blake,[4] R. J. Foley,[1] S. Jha,[1] E. Ramirez-Ruiz,[2,3,5]
J. Granot,[5,6] A. V. Filippenko,[1] S. Sigurdsson,[7] A. J. Barth,[8] H.-W. Chen,[9] M. C. Cooper,[1]
E. E. Falco,[4] R. R. Gal,[10] B. F. Gerke,[11] M. D. Gladders,[12] J. E. Greene,[4] J. Hennanwi,[1,13]
L. C. Ho,[12] K. Hurley,[14] B. P. Koester,[15] W. Li,[1] L. Lubin,[10] J. Newman,[13,16]
D. A. Perley,[1] G. K. Squires,[17] AND W. M. Wood-Vasey[4]

ABSTRACT

The localization of the short-duration, hard-spectrum gamma-ray burst GRB 050509b by the *Swift* satellite was a watershed event. We report the discovery of the probable host galaxy, a bright elliptical galaxy at $z = 0.2248$. This is the first known redshift and host of a short-hard GRB and shows that at least some short-hard GRBs are cosmological in origin. We began imaging the GRB field 8 minutes after the burst and continued for 8 days. We present a reanalysis of the XRT afterglow and report the absolute position of the GRB. Based on positional coincidences, the GRB and the elliptical are likely to be physically related, unlike any known connection between a long-duration GRB and an early-type galaxy. Similarly unique, GRB 050509b likely also originated from within a rich cluster of galaxies with detectable diffuse X-ray emission. We demonstrate that while the burst was underluminous, the ratio of the blast wave energy to the γ-ray energy is consistent with that of long-duration GRBs. Based on this analysis, on the location of the GRB (40 ± 13 kpc from the putative host), on the galaxy type (elliptical), and the lack of a coincident supernova, we suggest that there is now observational support for the hypothesis that short-hard bursts arise during the merger of a compact binary. We limit the properties of any Li-Paczyński "minisupernova" that is predicted to arise on ~1 day timescales. Other progenitor models are still viable, and new *Swift* bursts will undoubtedly help to further clarify the progenitor picture.

Subject heading: gamma rays: bursts

Online material: color figures

1. INTRODUCTION

The distribution in duration (Mazets et al. 1981; Norris et al. 1984) and hardness (Kouveliotou et al. 1993) reveals evidence for two distinct populations of classic gamma-ray bursts (GRBs): long-duration bursts, with typical durations around 30 s and peak energies at ~200 keV; and the minority, short-duration bursts, with durations of a few hundred milliseconds and harder spectra. Despite remarkable progress in understanding the nature and progenitors of long-duration GRBs, comparatively little has been learned about the origin of short-hard bursts, primarily because very few such bursts have had rapid and precise localizations.

The modeled bursting rate at redshift $z = 0$ of long-soft bursts outnumbers short-hard bursts by about a factor of 3.5 in the Burst and Transient Source Experiment (BATSE) catalog (Schmidt 2001); this assumes the same bursting rate as a function of redshift and does not include the effect of beaming, which, if different for long and short bursts, would imply that the intrinsic relative rates differ from those observed. While a number of bursts have been triangulated through the Interplanetary Network (see Hurley et al. 2005b) on roughly day-long timescales, there has only been one precisely localized short-hard burst relayed to ground observers in less than 1 hr (GRB 050202, *Swift*; Tueller et al. 2005);[18] owing to its proximity to the Sun at the time of localization, sparse ground-based follow-up was undertaken. Including GRB 050509b, this corresponds to a ratio of 1:18 for short-hard to long-soft burst detections with *Swift*, much smaller than the BATSE result.[19]

As with long-duration bursts, the distribution of short bursts appears very nearly isotropic (Kouveliotou et al. 1993; Briggs et al. 1996), and their brightness distribution ($\langle V/V_{max} \rangle \approx 0.35$) is

[1] Department of Astronomy, 601 Campbell Hall, University of California, Berkeley, CA 94720-3411.

[2] University of California Observatories/Lick Observatory, University of California, Santa Cruz, CA 95064.

[3] Chandra Fellow.

[4] Harvard-Smithsonian Center for Astrophysics, 60 Garden Street, Cambridge, MA 02138.

[5] Institute for Advanced Study, Olden Lane, Princeton, NJ 08540.

[6] KIPAC, Stanford University, P.O. Box 20450, Mail Stop 29, Stanford, CA 94309.

[7] Department of Astronomy and Astrophysics, 525 Davey Laboratory, Pennsylvania State University, University Park, PA 16802.

[8] Department of Physics and Astronomy, 4129 Frederick Reines Hall, University of California, Irvine, CA 92697-4575.

[9] Center for Space Research, Massachusetts Institute of Technology, Cambridge, MA 02139-4307.

[10] Department of Physics, 1 Shields Avenue, University of California, Davis, CA 95616-8677.

[11] Department of Physics, 366 LeConte Hall, University of California, Berkeley, CA 94720-7300.

[12] Carnegie Observatories, 813 Santa Barbara Street, Pasadena, CA 91101.

[13] Hubble Fellow.

[14] Space Sciences Laboratory, 7 Gauss Way, University of California, Berkeley, CA 94720-7450.

[15] Department of Physics, University of Michigan, Ann Arbor, MI 48109-1090.

[16] Institute for Nuclear and Particle Astrophysics, Lawrence Berkeley National Laboratory, Berkeley, CA 94720.

[17] *Spitzer* Science Center, Mail Stop 314-6, California Institute of Technology, Pasadena, CA 91125.

[18] There have been a few other short bursts (duration ≲2 s) detected and well localized, but with soft spectra and hence not members of the short-hard class. For example, GRB 040924 was a soft, X-ray–rich GRB (Fenimore et al. 2004; Huang et al. 2005). Hereafter, we use the term "short burst" interchangeably with short-hard burst.

[19] As of 2005 May 20, *Swift* has localized two short bursts out of a total of 38; see http://swift.gsfc.nasa.gov/docs/swift/archive/grb_table.html.

consistent with being a cosmological population. Still, there is no strong evidence to support the idea that short bursts are preferentially seen from $z \lesssim 0.37$ rich Abell clusters (Hurley et al. 1997), nor are they clearly connected with star formation within $\sim$100 Mpc (Nakar et al. 2005).

Without precise and rapid localizations, the population statistics do not provide a strong constraint on the short-burst progenitors. Still, it has been largely reckoned that the leading candidates for short bursts are the merger of a neutron star (NS) binary (NS-NS; Blinnikov et al. 1984; Paczyński 1986, 1991; Narayan et al. 1992; Katz & Canel 1996; Ruffert & Janka 1999; Rosswog & Ramirez-Ruiz 2002; Rosswog et al. 2003) or a black hole–neutron star binary (BH-NS; Lattimer & Schramm 1976; Eichler et al. 1989; Mochkovitch et al. 1993; Kluzniak & Lee 1998; Bethe & Brown 1999; Popham et al. 1999; Fryer et al. 1999). These systems hold several particular attractions. First, although uncertain, the estimated rate of mergers (between 1.5 and 20 per 10^6 yr per galaxy; Belczynski et al. 2002; Sipior & Sigurdsson 2002; Rosswog et al. 2003) is comparable to the short-burst rate (Schmidt 2001). Second, the dynamical timescale of such mergers is several milliseconds, and the sound-crossing times are of the order 10 ms, comparable to the shortest observed bursts (Miller 2005). Third, compact merger systems are likely to contain enough mass energy in a transient torus to power short-burst fluences as would be observed if at cosmological distances (Rosswog et al. 2003; Lee et al. 2004; Rosswog 2005). The typical dynamical timescale in such binaries immediately prior to coalescence (i.e., milliseconds) is much shorter than the observed burst duration, so it requires the central engine to evolve into a configuration that is stable, while retaining a sufficient amount of energy to power the burst (Lee et al. 2004).

Mergers of such compact remnants are by no means the only possible channel to produce short bursts. Evaporating primordial black holes may produce short ($<$100 ms) GRBs (Cline et al. 1999), although basic energetics arguments suggest that it would be difficult to see such sources from distances well beyond the Galaxy. The recent discovery of a megaflare from SGR 1806$-$20 (Mereghetti et al. 2005; Hurley et al. 2005a; Palmer et al. 2005; Terasawa et al. 2005) led to plausible suggestions that a substantial fraction ($\approx$40%) of short bursts could be produced by extragalactic magnetars (Hurley et al. 2005a). However, positional (Palmer et al. 2005; Nakar et al. 2005) and spectral (Lazzati et al. 2005) arguments have led other workers to suggest that at most a few percent of the BATSE catalog could consist of short-burst magnetars. Note that not all compact mergers create fertile conditions (a transient torus around a BH) for making a short burst (e.g., Janka & Ruffert 2002; Rosswog et al. 2004). The duration of the burst in a compact binary merger is determined by the viscous timescale of the accreting gas, which is significantly longer than the dynamical timescale, thus accounting naturally for the large difference between the durations of bursts and their fast variability (Lee et al. 2004). In the collapsar scenario for long-duration bursts, on the other hand, the burst duration is given by the fall-back time of the gas (Woosley 1993; MacFadyen & Woosley 1999), which is typically greater than a few seconds. However, a modified collapsar scenario in which the burst duration is determined not by fall-back but rather by the dynamical timescales associated with the expanding outflow might still meet the constraints of short GRBs (Woosley 2001).

The theoretical predictions for the afterglows of short GRBs have been considered by Panaitescu et al. (2001). Since the peak flux of the prompt emission is comparable for short and long GRBs, if their distance scales are similar the isotropic equivalent energy output in gamma rays ($E_{\gamma,\mathrm{iso}}$) would be proportional to the duration of the GRB, which is $\sim$10–100 times larger for long GRBs. If the efficiency for producing the gamma rays is comparable, then the isotropic equivalent kinetic energy in the afterglow shock ($E_{k,\mathrm{iso}}$) would have a similar ratio between long and short GRBs. This would imply the afterglow of short GRBs to be on average $\sim$10–40 times dimmer in flux than that of long GRBs. The afterglows of short GRBs would even be much dimmer than this if they encounter a much smaller external density compared to long GRBs; this is the expectation from short bursts from binary mergers outside of the host galaxy. Panaitescu et al. (2001) argued that a low external density would not affect the X-ray band, as the latter was assumed to lie above the cooling-break frequency, ν_c. We find that for a very low external density the electron cooling becomes very slow so that ν_c can lie above the X-ray band for the first few days, thus reducing the X-ray flux compared to that for a higher external density typical of the interstellar medium (ISM) found near star-forming regions of long-duration GRBs.

To date, the deepest early-time observations ($\Delta t \lesssim 1$ hr) yielded upper limits $V_{\mathrm{lim}} \approx 14$ mag from the 0.3 m Robotic Optical Transient Search Experiment (ROTSE-I; Kehoe et al. 2001). Hurley et al. (2002) compiled deeper nondetections at optical and radio wavelengths at times from days to weeks after four short bursts, with the faintest nondetection of $R \approx 22.3$ mag at $\Delta t = 20$ hr (see also Gandolfi et al. 2000). Clearly, deep and early observations in search of a short-burst afterglow would require a rapid localization to an uncertainty comparable to the field of view of meter class (and larger) telescopes.

GRB 050509b (Gehrels et al. 2005) triggered the BAT coded-mask imager on board *Swift* on 2005 May 9 04:00:19.23 (UT dates and times are used throughout this paper; Hurkett et al. 2005). The position of GRB 050509b, with an uncertainty of $4'$ radius, was relayed to the ground within a few seconds. The initial localization was later revised to a position of R.A. = $12^\mathrm{h}36^\mathrm{m}18^\mathrm{s}$, decl. = $+28°59'28''$, with a 95% confidence error radius of $2'.8$ (Barthelmy et al. 2005). Barthelmy et al. (2005) describe the burst as a single-peaked source with duration of $\sim$30 ms, peak flux of 2100 counts s^{-1} (15–350 keV), and a hardness ratio consistent with that of the short-hard population. At 06:29:23, a fading X-ray source was reported with a $6''$ localization (Kennea et al. 2005) and later updated to an $8''$ uncertainty radius at the position R.A. = $12^\mathrm{h}36^\mathrm{m}13^\mathrm{s}.9$, decl. = $+28°59'01''$ (Rol et al. 2005).

GRB 050509b thus represents the first short-hard burst localized in real time to a position suitable for immediate follow-up observations from a suite of ground-based facilities. In this paper we describe the results of our observations of the field of GRB 050509b and what bearing these data have on the nature of short bursts and the physics of short-burst afterglows. In § 2 we describe imaging and spectroscopy of the field. Our analysis of the X-ray afterglow of GRB 050509b is given in § 3, leading to a localization near an elliptical galaxy (§ 4). In § 5 we present a spectrum of that galaxy, its redshift, and inferred properties. We then argue, on statistical grounds, for a plausible association of this galaxy and the GRB. We demonstrate in § 6 how GRB 050509b appears to be a subluminous burst relative to long-duration GRBs, but with a ratio of blast wave energy to gamma-ray energy that is consistent with the long-duration population. In the remaining sections we describe new constraints on the nature of short-burst progenitors. Throughout, we assume a concordance cosmology with $H_0 = 70$ km s^{-1} Mpc^{-1}, $\Omega_\Lambda = 0.7$, and $\Omega_m = 0.3$. All of the results presented herein, although generally consistent with our previous results in GCN Circulars, supersede them.

2. OBSERVATIONS AND REDUCTION

Initially, several groups (Rykoff et al. 2005; de Ugarte Postigo et al. 2005; Bloom et al. 2005a; Torii 2005) reported no new optical/infrared source that was consistent with the XRT position of GRB 050509b (Kennea et al. 2005). At 07:21:27 we highlighted the proximity of the XRT to a bright red galaxy (2MASX J12361286+2858580, hereafter G1) and suggested a plausible physical association (Bloom et al. 2005a) based on its presumed membership in a $z \approx 0.22$ cluster (Barthelmy et al. 2005). We later reported the determination of the redshift in Prochaska et al. (2005a, 2005b). At 08:44:13 we noted the presence of a faint, compact source (hereafter S1; see Fig. 1) in the outskirts of G1, which we deemed a plausible candidate counterpart (Bloom et al. 2005b). A very similar suggestion was made at 09:36:49 by Cenko et al. (2005a); in addition, they noted apparent variability of the candidate (later retracting the variability claim, in Cenko et al. 2005c) and detection of three other faint sources (S2–S4) consistent with the XRT position (see also Cenko et al. 2005b). Two additional sources (S5 and S6) in the XRT location were subsequently noted from Very Large Telescope (VLT) imaging by Hjorth et al. (2005b), followed by another five sources (J1–J5) reported by Bloom et al. (2005c). No radio emission (Saz Parkinson 2005; van der Horst et al. 2005) or GeV/TeV emission (Soderberg & Frail 2005) is consistent with the XRT error localization. Below we discuss the observations, and further interpretation, leading to these reports.

2.1. *Optical and Infrared Imaging*

We observed the field of GRB 050509b on May 9 with the Wisconsin-Indiana-Yale-NOAO (WIYN) 3.5 m telescope and the OPTIC CCD imager with a $9.'6 \times 9.'6$ field of view and a plate scale of $0.''14$ pixel^{-1}. Under poor ($\sim 2''$) seeing conditions, two exposures totaling 360 s were obtained in the i' band beginning at 04.344 hr. In addition, we obtained 2400 s of integration in the r' band under improved seeing conditions ($\sim 1''$) beginning at 06.088 hr.

The data were reduced in the usual manner, using flat fields from both the illuminated dome and the twilight sky. The astrometric solutions to the individual images were calculated by comparison to the USNO-B1.0 catalog with a rms residual of $0.''1$. The photometric zero points of the images were calculated by comparison to more than 50 stars in the Sloan Digital Sky Survey (SDSS) photometry provided by Eisenstein et al. (2005). The zero points of the WIYN images are uncertain at about the 3% level. Limiting magnitudes were estimated from the histogram of fluxes in 10^4 seeing-matched apertures placed randomly within the field. The dispersion (σ) of a Gaussian fitted to this distribution was used to estimate the 5 σ limiting flux in each image, which was converted to a magnitude using the known zero point.

The bright galaxy G1 to the west of the XRT position contaminates a significant portion of the $8''$ radius XRT error circle. We used `galfit` (Peng et al. 2002) to fit a smooth Sérsic profile to this galaxy, in order to remove most of the contaminant light prior to examining the XRT error circle. A series of 1000 seeing-matched apertures placed randomly within the XRT error circle identified no new sources. The faint galaxy S1 was detected at the $>5 \sigma$ level in our deeper r' images.

Near-infrared images were obtained with the 1.3 m Peters Automated Infrared Imaging Telescope (PAIRITEL) in the J, H, and K_s bands (see Blake et al. 2005). Observations consisted of a 1130 s integration comprising 7.8 s dithered exposures beginning at 04.1375 hr. These data were reduced by median-
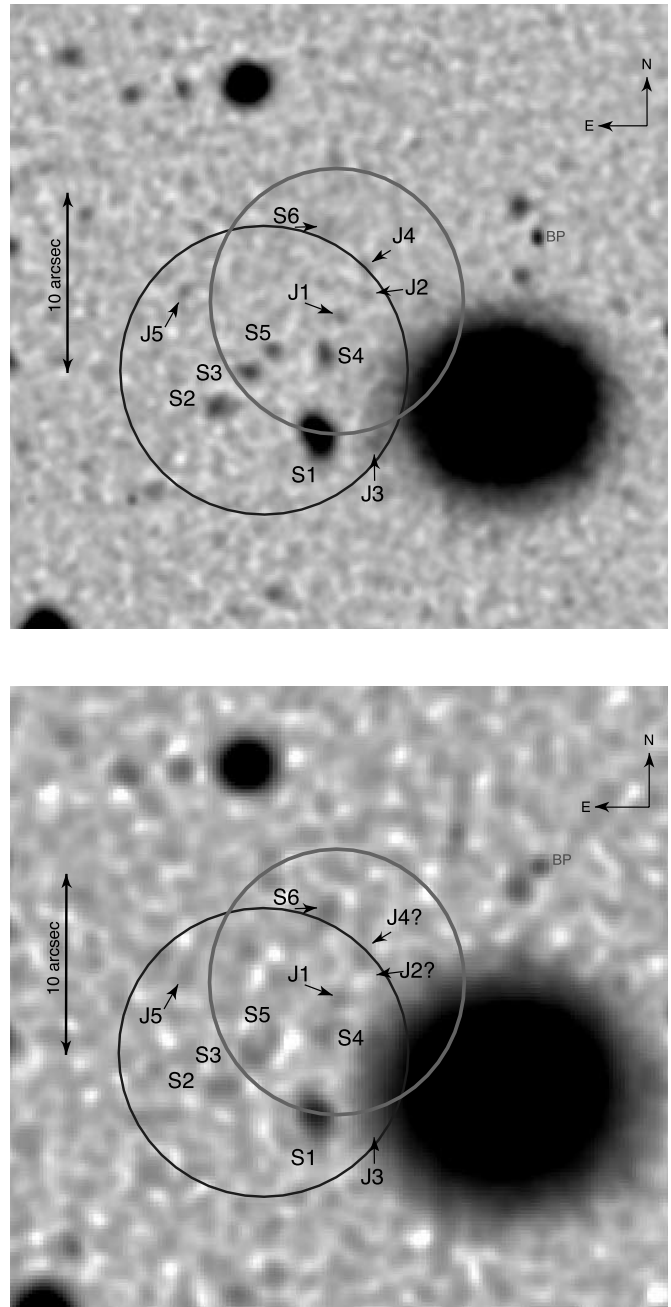

Fig. 1.—Keck LRIS G-band (*top*) and R-band (*bottom*) images, zoomed to show the XRT error circle. The larger, lower circle is the revised XRT position from Rol et al. (2005); the smaller, upper circle to the west and north of that is our 2 σ confidence region (see text) of the XRT position. The images have been median-subtracted and smoothed to accentuate the detection of faint sources under the glare of the bright galaxy G1. The 11 sources consistent with the Rol et al. (2005) X-ray afterglow localization are labeled in both images, with the astrometric positions given in Table 2. North is up and east is to the left. G1 is the large galaxy to the west and south of the XRT. Bad pixel locations are denoted with "BP." [*See the electronic edition of the Journal for a color version of this figure.*]

combining sets of individual exposures within a moving 5 minute window. The resulting median was used to subtract the bright sky from the individual images. Finally, all of the individual images were combined to make high-resolution mosaics using a modified version of `drizzle` (Fruchter & Hook 1997). Zero points were determined 2MASS stars in the field. Upper limits in the JHK_s mosaics were estimated using the same
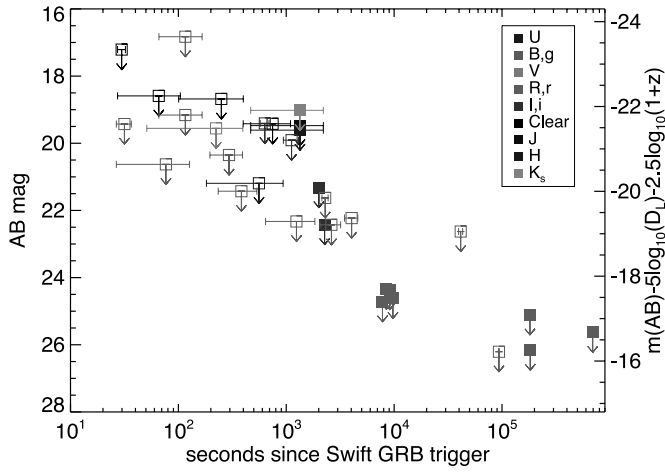
Fig. 2.—Upper limits from WIYN, PAIRITEL, and Keck images (*filled squares*) along with those reported in the literature (*open squares*). Magnitudes are corrected for extinction using the maps of Schlegel et al. (1998) and converted to AB magnitudes, assuming $z = 0.2248$ (see text), using the relations of Frei & Gunn (1994) and Blanton et al. (2003a). Times are reported in seconds relative to the *Swift* trigger on 2005 May 9.166889. The WIYN and PAIRITEL upper limits are 5 σ, but many of the quoted limits in the literature are not accompanied by a stated significance level. For smaller telescopes with large pixels, the light from the nearby galaxy is likely a significant contaminant, resulting in upper limits that may be overestimated in the literature. [*See the electronic edition of the Journal for a color version of this figure.*]

technique as for the WIYN data. The WIYN and PAIRITEL upper limits, as well as limits reported in the literature, are shown in Figure 2.

We later imaged the field of GRB 050509b with the Keck I 10 m telescope and the Low Resolution Imaging Spectrograph (LRIS-B; Oke et al. 1995), using the dichroic D560 (50% transmission point at 5696 Å) with G and R filters. Starting at 2005 May 11.25, near astronomical twilight, we took five dithered images in each band for a total of 1660 and 1620 s exposures in G and R, respectively. The data were reduced in the usual manner and combined, weighted by exposure times.

On 2005 May 17 08:05.5, 8.17 days after the GRB, we obtained deep R (Ellis—which is similar to Harris R; Bacon et al. 2003) imaging on the Echellette Spectrograph and Imager (ESI; Sheinis et al. 2002) on the Keck II 10 m telescope. In the presence of bright glare from the Moon, we combined several reduced images for an effective exposure time of 960 s. Since there is a negligibly small color term in converting Harris R to R_C,[20] we found a zero point relative to the LRIS R image. There are no new sources to $R_C \approx 25.0$ mag (5 σ), nor significant variations of the faint sources in the XRT error circle. Table 1 summarizes the photometric limits.

[20] See http://www.ast.cam.ac.uk/~wfcsur/technical/photom/colours.

TABLE 1
Upper Limits on Optical-IR Afterglow of GRB 050509b

Start Time[a] (s)	Exposure Time (s)	Band	Limit[b] (AB mag)	References
467.8	1741	J	19.3	This work
467.8	1741	H	19.5	This work
467.8	1741	K_s	18.95	This work
1973.6	60	i	20.95	This work
2118.3	300	i	22.05	This work
7497.3	600	r	24.21	This work
8172.3	600	r	23.84	This work
8808.3	600	r	23.85	This work
9446.9	600	r	24.11	This work
179696	1260	R	24.6	This work
179696	1260	G	25.5	This work
691200	960	R	25.1	This work
27.3	5	Clear	17.21	Rykoff et al. (2005)
27.3	77	Clear	18.59	Rykoff et al. (2005)
100.6	299	Clear	18.68	Rykoff et al. (2005)
399.1	696	Clear	19.42	Rykoff et al. (2005)
26.6	10	R	18.92	Wozniak et al. (2005)
26.6	100	R	20.12	Wozniak et al. (2005)
234	300	R	20.92	Wozniak et al. (2005)
643	1200	R	21.82	Wozniak et al. (2005)
2052	1140	R	21.92	Wozniak et al. (2005)
3466	1140	R	21.72	Wozniak et al. (2005)
66	100	B	18.34	Sasaki et al. (2005)
66	100	R	16.32	Sasaki et al. (2005)
2142.9	300	R	21.12	de Ugarte Postigo et al. (2005)
572.9	120	I	19.04	Torii (2005)
939.9	360	I	19.54	Torii (2005)
51	345	V	18.96	Breeveld et al. (2005)
196	197	B	20.14	Breeveld et al. (2005)
182	753	U	19.4	Breeveld et al. (2005)
39600	3600	R	22.12	Misra & Pandey (2005)
93240	900	R	25.7	Cenko et al. (2005c)

[a] Time since 04:00:19 UT, the time of the *Swift* BAT trigger.
[b] Limits were converted to AB magnitudes following Frei & Gunn (1994). Limits are presumed to be 5 σ detection limits for a point source (not all reports in the literature stated the significance of the upper limits). No extinction correction has been applied to these magnitudes.

3. THE X-RAY EMISSION

The *Swift* XRT (Burrows et al. 2000) began observations of GRB 050509b on 2005 May 9 at 04:00:56, approximately 61 s after the BAT trigger. The observations consisted of 11 blocks, each about 2.5 ks in duration (except the first observation of 1.6 ks and the last observation of 1.8 ks), spread over a period of $\sim$21 hr. The XRT operated in a number of different modes throughout the observations. The most common (32.3 ks of exposure) and most useful mode for this object was the "Photon Counting" mode, which retains the full imaging and spectroscopic resolution of the instrument. The images are 480×480 pixels, with a scale of $2\rlap{.}''36$ pixel^{-1}. The XRT point-spread function is energy-dependent, with a half-power diameter of $18''$ at 1.5 keV. The energy resolution is also a function of energy, varying from about 50 eV at 0.1 keV to about 190 eV at 10 keV.

The first Photon Counting observation began at 04:01:20 (Kennea et al. 2005) and lasted 1640 s. As noted in Kennea et al. (2005) and Rol et al. (2005), a faint X-ray source is detected in this first of 11 observations, but it faded quickly below the background. We have obtained the XRT data from the *Swift* archive and have analyzed them to determine the position of this X-ray afterglow candidate, as well as to examine its variability. We briefly review the data reduction, and then we discuss the localization of the afterglow candidate and attempt to quantify the decay.

3.1. *Swift Data Reduction*

Using the Level 1 data from the *Swift* archive, we ran the `xrtpipeline` script packaged with the HEAsoft 6.0 software supplied by the NASA High Energy Astrophysics Science Archive Research Center.[21] We used the default grade selection (grades 0 to 12) and screening parameters to produce a Level 2 event file recalibrated according to the most current (as of 2005 May 15) calibration files in the *Swift* database.[22] To produce images for source detection, we used the XSELECT software (also part of HEAsoft 6.0), with a filter to include only counts in PI channels 30–1000 (corresponding to photon energies of 0.3–10 keV). The PI channel to photon energy conversion was accomplished with the redistribution file swxpc0to12_20010101v007.rmf from the calibration database. The effective area of the XRT at the position of the afterglow candidate was determined with the `xrtmkarf` tool, using the correction for a point source.

3.2. *X-Ray Afterglow Localization*

A number of factors make the localization of this X-ray afterglow difficult. It is intrinsically faint and superposed on diffuse X-ray emission from a galaxy cluster at $z = 0.22$ (Gal et al. 2003). The initial source detection was performed with the wavelet-based routine `wavdetect` (Freeman et al. 2002), supplied with the CIAO 3.2 software package, which in our experience is quite good at detecting faint sources. We chose parameters appropriate for detecting point sources in this XRT observation; the pixel scales considered were a $\sqrt{2}$ series starting at 4 pixels (4, 5.657, 8, 11.314, and 16), and the significance threshold was set at 4×10^{-6}, corresponding to a $\sim$1 false positive detection of a point source in the image. We detect 22 compact sources in the entire 32.3 ks data set.

To study the properties of the afterglow candidate, we extracted all of the events within an area of radius 10 pixels around the nominal `wavdetect` position. In the first observation of 1.6 ks,
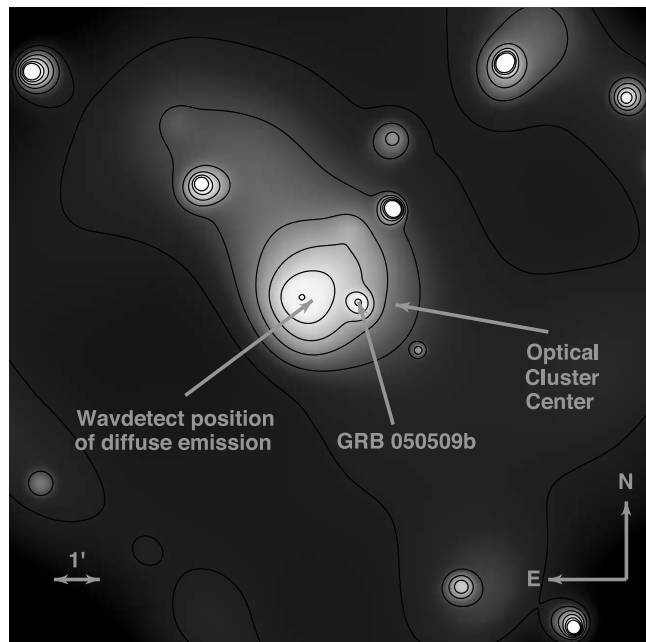

Fɪɢ. 3.—A $14' \times 14'$ adaptively smoothed image of the XRT data. GRB 050509b is embedded in the diffuse X-ray emission associated with the galaxy cluster and is about 270 kpc in projection from the cluster center. [*See the electronic edition of the Journal for a color version of this figure.*]

there are 14 counts in this region. When examining a plot of the cumulative distribution versus time, we noticed that the majority of the counts from this region occurred in the first 300 s. We therefore further investigated this brief interval.

In the first 300 s of the first Photon Counting observation, the XRT detected 92 counts on the entire chip, with 73 of them outside of the 22 source regions. Within any 10 pixel radius source region, we therefore expect an average of 0.1 background counts. We detect nine counts in this region of the X-ray afterglow, with a reasonable expectation that all nine are from the X-ray afterglow. Using the mean location of just these nine counts, we can obtain a relatively uncontaminated estimate of the source position. We calculate the 68% confidence interval in each direction as $T\sigma_j/\sqrt{N}$, where N is the number of counts (9), σ_j is the sample standard deviation of the nine coordinates in each direction, and $[-T, T]$ is the 68% confidence interval of the Student's t distribution with $N - 1$ degrees of freedom. This gives us a position estimate, *in the Swift XRT reference frame*, of R.A. = $12^{\mathrm{h}}36^{\mathrm{m}}13\rlap{.}^{\mathrm{s}}94$, decl. = $+28°59'05\rlap{.}''3$ (J2000), with an uncertainty of $3\rlap{.}''6$ in right ascension and $3\rlap{.}''5$ in declination. This is $4\rlap{.}''3$ north of the revised XRT position reported by Rol et al. (2005). A possible reason for this offset is that the Rol et al. position is based on 6.6 ks of XRT exposure and thus includes contributions from the diffuse cluster emission (see Fig. 3), biasing the position estimate.

We examine the absolute astrometric accuracy of the *Swift* XRT frame by searching for possible counterparts of the other 21 XRT sources in deep optical images. The best-suited image for this is a *B*-band exposure from the 2.3 m Bok telescope (Engelbracht & Eisenstein 2005), because it covers an area large enough to contain the entire XRT field. Using a cross-correlation to 250 2MASS positions, we fit an absolute world coordinate system (WCS) using IRAF/CCMAP.[23] The overall geometry plus the considerable
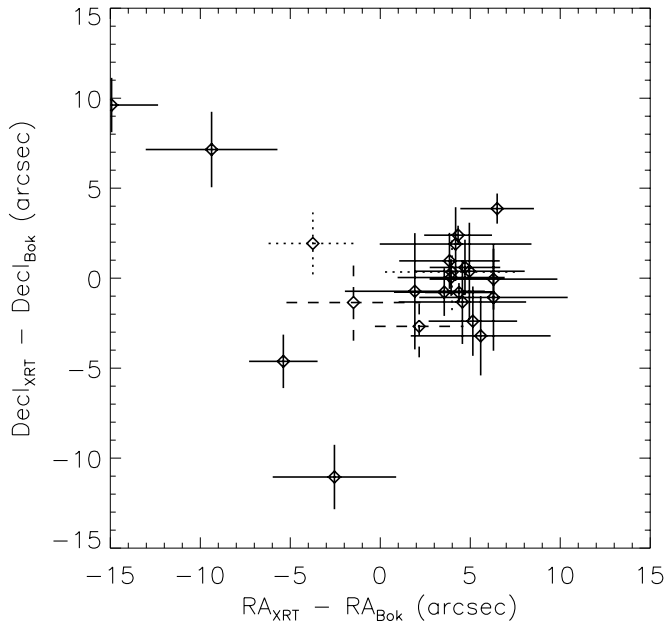
FIG. 4.—Scatter plot of the position offsets between the XRT sources (other than the afterglow candidate) and their nearest sources in the wide-field Bok B-band image. Two of the XRT sources each have two Bok sources nearby. For these two XRT sources, the dashed line represents the offset to the closest source, and the dotted line represents the offset to the next closest source. There is strong clustering around an offset of 4″.5 in right ascension, indicating a global shift in the absolute astrometric zero point of the XRT frame. The number of X-ray/optical cross matches is reasonable given the sensitivity of the two frames (see text).

distortion across the Bok B-band image was well fit by a fourth-order polynomial with rms residuals of 0″.135 in right ascension and 0″.158 in declination. Assuming a 100 mas global uncertainty in the 2MASS International Celestial Reference System (ICRS) tie, the absolute astrometry in the wide-field optical frame is thus uncertain to 170 mas in right ascension and 187 mas in declination.

For each XRT source other than the afterglow candidate, Figure 4 plots the offset between the XRT position and the position of the closest optical source. Two XRT sources had two optical sources within 5″; for these, the closest optical source is represented by dashed lines, and the next closest is represented by dotted lines. There is an obvious locus around a 4″.5 difference in right ascension, suggesting that these XRT sources are associated with the corresponding nearest optical sources. At a detection sensitivity around 10^{-14} ergs cm^{-2} s^{-1}, it is not surprising to find so many optical counterparts in the moderately deep Bok image. In a *Chandra*/Subaru study of the R.A. = 13 hr *XMM-Newton*/*Röntgensatellit* (*ROSAT*) field, McHardy et al. (2003) find unambiguous optical counterparts for 61 of the 66 X-ray sources above 10^{-14} ergs cm^{-2} s^{-1}. The mean R magnitude of these sources is $\bar{R} = 20.7$, and the faintest counterpart is at $R = 24.4$ mag.

Using the 14 sources in the above locus (excluding the two sources with multiple possible counterparts), we derive an offset between the XRT frame to the optical frame of 4″.49 ± 0″.72 west in right ascension and 0″.42 ± 0″.30 south in declination. Our best estimate for the location of the X-ray afterglow is therefore R.A. = $12^h36^m13^s59$, decl. = $+28°59'04″.9$ (J2000); this is 4″.1 west and 3″.9 north of the revised XRT position reported in Rol et al. (2005). The uncertainty in our position is a combination of the statistical uncertainty of the XRT localization (3″.6 in right ascension, 3″.5 in declination) and the uncertainty in shifting the XRT frame to the ICRS (0″.76 in right ascension, 0″.40 in declination).

The astrometry in our original reports from WIYN and Keck imaging was based on a frame of approximately 10 stars in the 2MASS catalog. The release of the SDSS data and calibrations of this field allow us to improve the astrometric tie to the ICRS. We fit the Keck LRIS G-band image to 91 sources in common with the SDSS object catalog with a third-order polynomial solution using IRAF/CCMAP. The uncertainty in the astrometric tie to SDSS, based on residuals from the fit, is σ(R.A.) = 0″.134 and σ(decl.) = 0″.153. Assuming a 75 mas astrometric uncertainty in the SDSS astrometric calibration to the ICRS (Pier et al. 2003), we estimate that the absolute uncertainty in the Keck ICRS tie is σ(R.A.) = 0″.154 and σ(decl.) = 0″.171.

The XRT location is 11″.2 ± 3″.6 (or 40 ± 13 kpc in projection) from G1, as we first noted in Bloom et al. (2005a). Spectroscopy of this source reveals that it is indeed an early-type galaxy (see § 5) and is a member of a cluster, NSC J123610+285901, at $z \approx 0.22$ (Gal et al. 2003; Barthelmy et al. 2005). Near the location of the revised XRT error circle, we find $\sim$11 faint sources (all of which we or others have reported previously; see above). Figure 1 shows the Keck G and R images with the identified source labeled. Table 2 gives the astrometric positions and magnitudes of the sources.

3.3. *X-Ray Afterglow Decay*

We examine the first 1.6 ks block of observations to characterize the temporal properties of the X-ray afterglow. A Kolmogorov-Smirnoff (K-S) test on the arrival times of the 14 photons gives a probability of 0.06% that they come from a source with a constant count rate. The next step in model complexity is one in which the X-ray count rate R_X in this region has a constant component (due to the background and diffuse cluster emission) plus a component with a power-law dependence on time (due to the fading afterglow). Our model is thus $R_X(t) = A(t - t_0)^{-\alpha} + B$, where B is the constant (background plus cluster) count rate, t_0 is the time of the BAT trigger, and A is a normalization chosen such that the model preserves the detected flux over the 1.6 ks under consideration. We determine B to be 0.00107 counts s^{-1} from the later observations.

We considered a range of α from 0 to 4 and computed the K-S probability of the observed data coming from the model for each value of α. The K-S probability was highest (97.8%) at $\alpha \approx 1.3$. For $\alpha \lesssim 1$ (0.77) and $\alpha \gtrsim 1.7$ (2.1), the K-S probability dropped below 32% (5%). For $\alpha = 1.3$, the normalization A is 22 counts s^{-1}. We can translate this to an energy-flux normalization by determining the conversion from counts to ergs cm^{-2}. We consider only the first 300 s of data for this determination in order to reduce contamination from the background. For each of the nine counts, we know its energy, as well as the effective area, of the XRT at that energy. The average is 3.14 × 10^{-11} ergs cm^{-2} count^{-1}. Our model for the X-ray flux (0.3–10 keV) of the afterglow only is then $F_X(t) = A'(t - t_0)^{-\alpha}$. For $\alpha = 1.3$, the normalization is $A' = 6.9 \times 10^{-10}$ ergs cm^{-2} s^{-1}. For example, the X-ray flux of the afterglow at $t = 200$ s after the BAT trigger for $\alpha = 1$, 1.3, and 1.7 is $F_X(200) = 5.8$, 7.0, and 6.5×10^{-13} ergs cm^{-2} s^{-1}, respectively.

Figure 5 shows, on a common scale, X-ray light curves for a number of GRBs and core-collapse supernovae. The location of the X-ray transient associated with GRB 050509b, when placed at $z = 0.2248$, is striking. While the slope of the transient agrees well with those of typical GRBs, its flux falls well below the typical long-GRB range. In fact, for any reasonable redshift (i.e., $z \lesssim 3$–5), GRB 050509b would still be significantly underluminous in its X-ray afterglow when compared to those of long-duration GRBs (see Fig. 5). For the assumed redshift of

TABLE 2
Properties of Faint Sources in the XRT Error Circle

| | Position[a] | | Magnitudes[b] | | |
Source	R.A.	Decl.	g'	r'	Comments
S1	12 36 13.677	+28 58 57.51	23.80 ± 0.12	22.80 ± 0.14	Marginally consistent with new XRT error circle
S2	12 36 14.100	+28 58 58.90	25.27 ± 0.15	24.59 ± 0.24	Outside new XRT error circle
S3	12 36 13.961	+28 59 00.87	25.79 ± 0.21	24.45 ± 0.21	
S4	12 36 13.642	+28 59 01.80	25.59 ± 0.17	25.52 ± 0.47	
S5	12 36 13.865	+28 59 02.05	25.76 ± 0.20	25.36 ± 0.39	
S6	12 36 13.629	+28 59 08.81	25.96 ± 0.19	24.46 ± 0.22	Red galaxy
J1	12 36 13.574	+28 59 03.84	∼27.1	∼25.1	
J2	12 36 13.464	+28 59 05.18	∼28	≳25.5	Marginal detection
J3	12 36 13.435	+28 58 56.88	26.14 ± 0.21	24.27 ± 0.29	Outside new XRT error circle
J4	12 36 13.471	+28 59 06.87	∼27.3	≳25.5	Marginal detection related to J2?
J5	12 36 14.237	+28 59 05.39	∼26.8	25.5 ± 0.4	Outside new XRT

Note.—Units of right ascension are hours, minutes, and seconds, and units of declination are degrees, arcminutes, and arcseconds.

[a] J2000; positions are based on image centroids and have been tied to the SDSS astrometric frame (see text). The absolute positional uncertainty, inherited in part from the SDSS uncertainties, is 0″.2. The relative uncertainty between object positions is expected to be ∼0″.1.

[b] Photometry has been tied to the SDSS calibrations of the field. We used a color term in the conversion of the Keck R to the Sloan r' filter and constant magnitude offset (following Windhorst et al. 1991). We assumed no color term in converting G to g'. Errors include the 0.1 mag zero-point uncertainty in the tie to the SDSS photometry. We do not report photometric errors for those sources near the detection limit, but such errors are likely to be of the order 50%. No extinction correction has been applied to these magnitudes.

the tentative host galaxy, the extrapolated X-ray luminosity at a few days, which is also consistent with the *Chandra* upper limit (Patel et al. 2005), is close to those seen in typical core-collapse supernovae.

3.4. Diffuse Galaxy Cluster Emission

We used `wavdetect` to search for large-scale structures in the full 32.3 ks XRT data set. The pixel scales searched were 20, 28.28, 40, 56.57, and 80. The center of the diffuse emission presumably associated with the galaxy cluster had a `wavdetect`-determined position of R.A. = $12^h36^m18^s.26$, decl. = $+28°59'06''.7$. Figure 3 shows an adaptively smoothed image (using the CIAO tool `csmooth`) of the XRT data with the cluster center and GRB indicated. The colors represent the 0.3–10 keV count density. Contours are drawn at 0.00449, 0.00646, 0.00934, 0.0136,
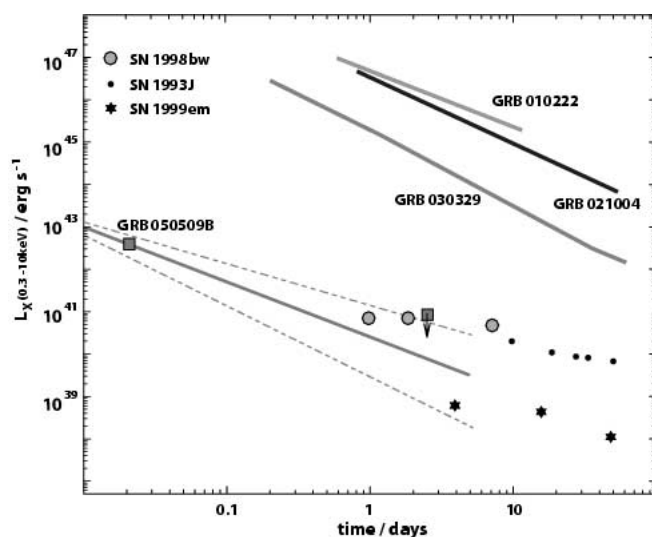

Fig. 5.—Compilation of observed X-ray light curves for GRBs and core-collapse supernovae (adapted from Kouveliotou et al. 2004). The X-ray luminosities for the short GRB 050509b are calculated assuming $z = 0.2248$. For GRB 050509b we used data points (*squares*) from both the XRT and the *Chandra* upper limit reported by Patel et al. (2005); the solid line corresponds to the best-fit temporal decay index of -1.3.

0.0197, and 0.0273 counts arcsec^{-2}. As the image shows, the `wavdetect`-determined position of the diffuse emission is about 14″ to the west and 4″ south of the peak of the diffuse emission, which is at R.A. = $12^h36^m19^s.33$, decl. = $+28°59'10''.8$ (J2000). (Note that the optical cluster center is R.A. = $12^h36^m10^s$, decl. = $+28°59'00''.9$ [J2000], as defined by the center of the galaxy over-density; this is about 125″ east and 10″ south of the peak of the diffuse X-ray emission.) We thus find that the XRT afterglow position is 75″ west, 6″ north of the cluster center, as defined by the peak of the diffuse X-ray emission, about 270 kpc in projection.

We extract a spectrum from a region of 110″ in radius, centered on the `wavdetect` position. We use a similar-sized region in a source-free area to extract a spectrum for background subtraction. We require the cluster spectrum to contain at least 20 counts per bin, and we consider the range 0.3–10 keV. We fit the background-subtracted cluster spectrum in XSPEC version 12.2 (Arnaud 1996) with a MEKAL (warm plasma) model absorbed by a Galactic column density of 1.52×10^{20} cm^{-2} (Dickey & Lockman 1990). We set the MEKAL redshift at $z = 0.2248$ and the metallicity at $[\mathrm{Fe/H}] = 0.26$ (Mushotzky & Loewenstein 1997) and allow the temperature and normalization to vary. The best-fit temperature is $kT = 5.25^{+3.36}_{-1.68}$ keV, which gives $\chi^2/\mathrm{dof} = 22.4/20$.

4. ASSOCIATING GRB 050509b WITH G1

We are now in a position to explore the possible association of GRB 050509b with the cluster and with the nearby elliptical galaxy G1. Focusing on the BAT localization alone, we first consider the probability that a random position in the sky would be in a rich cluster of galaxies (here we neglect the effects of lensing, expected to be small; see, e.g., Grossman & Nowak 1994). A reasonable estimate of the covering fraction of clusters on the sky is given by the Digitized Second Palomar Observatory Sky Survey (DPOSS) Northern Sky Optical Cluster Survey (Gal et al. 2003). Although this survey is not very deep ($z_{\mathrm{lim}} \sim 0.3$), low-redshift clusters should dominate the sky density. Gal et al. (2003) find a covering fraction of ∼0.03 assuming a typical cluster radius of 1 Mpc, which suggests a chance alignment is improbable but not impossible. Moreover, the XRT localization of GRB 050509b to within 45″ of the center of such a cluster would occur by chance

with a probability of just $\sim 7 \times 10^{-4}$, but it is difficult to estimate a posteriori how large a distance from a cluster center one would have considered "significant."

While the gas from the cluster environment may enhance the probability of localizing short-burst afterglows (see below), our expectation is that short GRB progenitors are caused by the death of stars of some sort, with the burst rate determined by processes on scales significantly smaller than cluster lengths. To this end, we should consider the chance probability of the GRB event occurring at close impact parameter to a galaxy similar to G1. As reported by Eisenstein et al. (2005), the galaxy G1 has a Petrosian r' magnitude of 17.18 ± 0.02 mag based on imaging by the SDSS. The sky density of galaxies with comparable apparent magnitude brighter than G1 is ~ 40 deg^{-2} (Blanton et al. 2003b). Therefore, the probability of an event randomly occurring within $20''$ (about twice the observed offset) of this bright galaxy is $\sim 5 \times 10^{-3}$. We consider this a conservative estimate because this probability makes no reference to the galaxy redshift, type, size, or age (which are consistent with a priori discussions of short-burst host galaxies; e.g., Bagot et al. 1998; Bloom et al. 1999).

If one argues that GRB 050509b is indeed physically associated with this bright, low-redshift elliptical galaxy, one must consider why the several other well-localized short bursts have not shown similar associations. The first possibility—that the short bursts arise from a more local population (as suggested by the magnetar flare from 2004 December 27; Hurley et al. 2005a) and that GRB 050509b must therefore arise from a different population—was discounted for four of the best-localized short bursts (Nakar et al. 2005). Another possibility is that GRB 050509b was significantly closer than the other well-localized short bursts. A strong test of this hypothesis is to determine if other short bursts are associated with more distant clusters or intrinsically bright, massive galaxies (e.g., through a deep imaging campaign). The third possibility is simply that short-burst progenitors need not always arise in such galaxies. In fact, for the NS-NS hypothesis we would expect mergers in galaxies spanning a wide range of Hubble types. A delayed BH-NS merger is also possible, but less likely if GRB 050509b is associated with G1: statistically, the distribution of timescales for BH-NS coalescence is as broad as that for NS-NS coalescence, albeit quite model-dependent (Belczynski et al. 2002; Sipior & Sigurdsson 2002), but the systemic kick velocity is expected to be systematically lower by a factor of a few in most theoretical models of formation of BH-NS binaries (kick velocity is roughly inversely proportional to mass, so more massive binaries receive less kick). Moreover, larger velocity kicks generally lead to shorter merger times. Thus, the ~ 40 kpc offset tends to favor NS-NS over BH-NS mergers.

While these possible associations are tantalizing, a posteriori statistics are very suspect. Had the GRB been near a bright spiral galaxy, we might have made similar claims based on chance probabilities. Nevertheless, it remains the case that many workers had predicted the distinct possibility that a well-localized compact merger and/or short burst could be near an elliptical galaxy (Bagot et al. 1998; Bloom et al. 1999; Panchenko et al. 1999; see also Livio et al. 1998), and so we suggest that these arguments might reasonably reflect a true association. Moreover, the possible association with an early-type host stands in stark contrast to results from long-duration GRBs (Bloom et al. 2002; Le Floc'h et al. 2003; Djorgovski et al. 2003) and is reminiscent (e.g., Bloom et al. 2002; Dar 2004) of the dichotomy between core-collapse and thermonuclear (Type Ia) supernovae. Only a larger sample of short GRBs will provide truly compelling evidence for such a

parallel. Still, based on the arguments above, we proceed by accepting the hypothesis that GRB 050509b is physically associated with G1.

5. A PUTATIVE HOST GALAXY AT $z = 0.2248$

We obtained a spectrum of G1 with the Deep Imaging and Multi-Object Spectrograph (DEIMOS; Faber et al. 2003) on the Keck II 10 m telescope under photometric conditions. The data were acquired in a series of two exposures starting at 07.47 hr on the night of the burst. The instrumental setup included the 600 line mm^{-1} grating blazed at 7500 Å and centered at 7200 Å, the GG455 order-blocking filter, and standard CCD binning. This setup gives nearly continuous wavelength coverage in the range 4500–9000 Å. We observed the galaxy through a $1\rlap{.}''1 \times 20''$ slit at sky position angle $90°$ and an air mass of 1.0. This setup yields a FWHM resolution of ~ 5 Å (i.e., $\sigma = 100$ km s^{-1}). The data were reduced and calibrated with the DEEP spectroscopic pipeline for DEIMOS data (M. Cooper et al. 2006, in preparation). Wavelength calibration and flat fielding were performed using spectra of Xe-Ne-Kr-Ar and quartz lamps (respectively) obtained that night.

The software provides a two-dimensional, sky-subtracted image of the spectrum across two CCDs of the DEIMOS mosaic. Unfortunately, the CCD that includes the bluest data has a pair of blocked columns that lie near the center of the galaxy profile. Therefore, we extracted the one-dimensional spectrum on this CCD using optimal extraction techniques, assuming a Gaussian profile with $\sigma = 9.2$ pixels (i.e., $1\rlap{.}''1$). For the other CCD, we extracted a one-dimensional spectrum by adopting a 26 pixel ($3''$) boxcar aperture. Finally, we processed and calibrated a spectrophotometric standard star (BD +28 4211) observed at the end of this night. After comparing its observed flux (in digital numbers) against the Space Telescope Imaging Spectrograph (STIS) CALSPEC calibration,[24] we calculated a sensitivity function that could be applied to our galaxy spectra.

Spectroscopic observations of G1, S1, S2, and two unidentified sources were obtained with the Gemini Multi-Object Spectrograph (GMOS; Hook et al. 2004) on the Gemini North 8 m telescope beginning at 2005 May 10.27 under photometric conditions. We used a $0\rlap{.}''75$ slit, an R400 grating blazed at 7640 Å, the GG455 order-blocking filter, and set the central wavelength to 6500 Å. The air mass was low (1.0–1.1), so the effects of atmospheric dispersion were negligible (Filippenko 1982). Standard CCD processing and spectrum extraction were accomplished with IRAF, using a $1\rlap{.}''74$ aperture for these sources of interest (S1, S2). The data were extracted using the optimal algorithm of Horne (1986). Low-order polynomial fits to calibration-lamp spectra were used to establish the wavelength scale. Small adjustments derived from night-sky lines in the object frames were applied. Using techniques discussed in Wade & Horne (1988) and Matheson et al. (2000), we employed IRAF and our own IDL routines to flux-calibrate the data and to remove telluric lines using the well-exposed continua of the spectrophotometric standard, EG 131 (Bessell 1999).

Figure 6 presents the one-dimensional flux-calibrated spectrum of G1 against a vacuum, heliocentric-corrected wavelength array. The dotted line traces a 1σ error array based on Poisson counting statistics. We have marked a number of detected absorption-line features and also the expected position for several strong transitions frequently observed in emission-line galaxies (e.g., Hα,
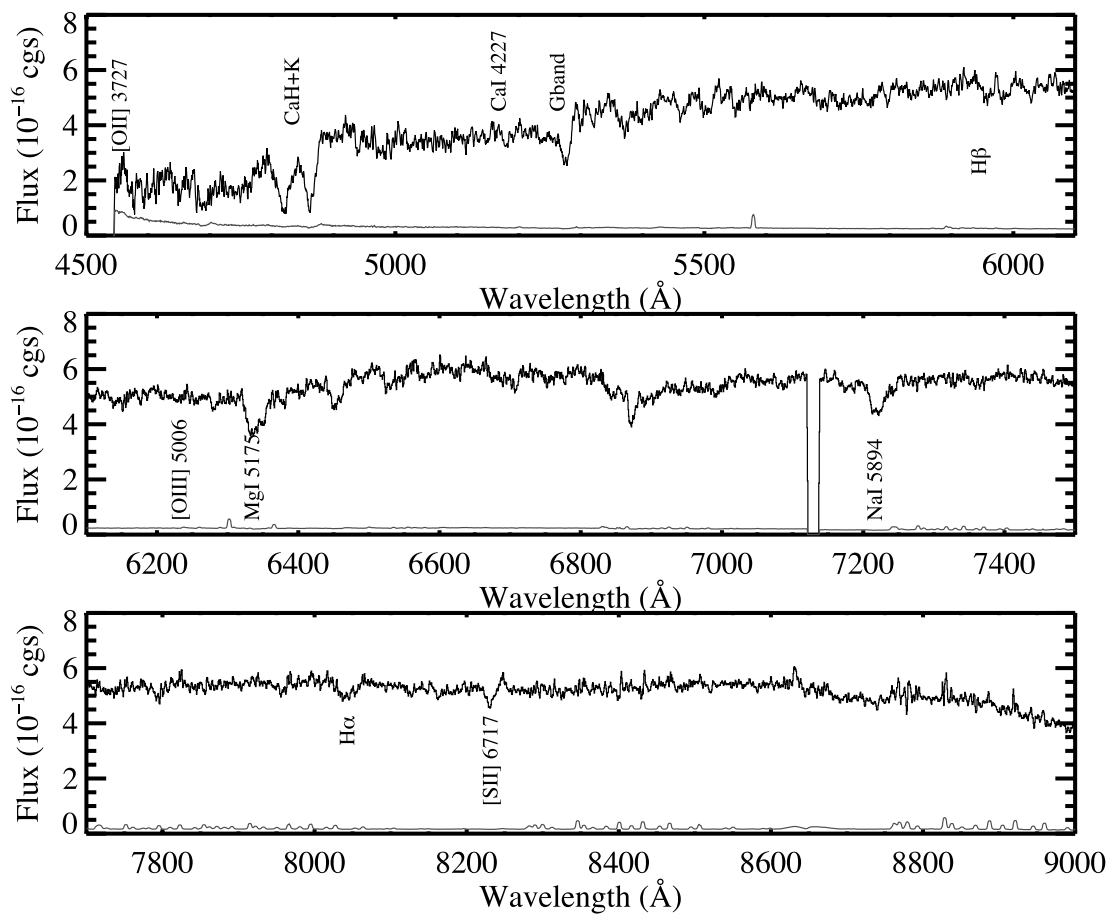
---

[24] See ftp://ftp.stsci.edu/cdbs/cdbs2/calspec.

FIG. 6.—Keck DEIMOS spectrum of the galaxy G1 (along with its variance spectrum) located ~10″ west of the center of the XRT error circle for GRB 050509b. The data were obtained using the 600 line mm^{-1} grating centered at 7200 Å, and the galaxy was observed through a 1″1 slit (FWHM ≈ 5 Å). The strong absorption-line features indicate $z = 0.2248$, and a comparison of the spectrum against a template spectrum of HD 72324 provides an estimate of the velocity dispersion: $\sigma = 260 \pm 40$ km s^{-1}. [*See the electronic edition of the Journal for a color version of this figure.*]

[O III]). We have fit a double Gaussian profile to Ca II H and K lines and measure $z = 0.2248 \pm 0.0002$. This is consistent with the redshift inferred photometrically for this cluster from DPOSS (Gal et al. 2003). At this redshift, the luminosity distance is 1117.4 Mpc, and 1″ corresponds to 3.61 kpc in projection.

To estimate the velocity dispersion of the galaxy, we have compared the spectrum against a template spectrum of HD 72324 (e.g., Kelson et al. 2000) smoothed by a wide range of σ. The best match to the absorption lines of G1 with $\lambda_{\rm rest} = 4000$–5300 Å is $\sigma = 275 \pm 40$ km s^{-1}. Accounting for the instrumental resolution, we derive a light-weighted velocity dispersion for this galaxy of 260 ± 40 km s^{-1}.

The spectral features evident in Figure 6 are typical of early-type galaxies. The spectral type and velocity dispersion indicate a massive elliptical galaxy with no apparent ongoing star formation. A quantitative limit to the current star formation rate (SFR) can be inferred from the upper limit to the Hα luminosity of this galaxy. The emission-line flux in a 10 Å window ($\Delta v \approx 300$ km s^{-1}) centered at the expected wavelength of Hα has a 3 σ upper limit of 1.2×10^{-16} ergs s^{-1} cm^{-2}. Adopting the current concordance cosmology, we derive an Hα luminosity $L_{\rm H\alpha} < 1.2 \times 10^{40}$ ergs s^{-1}. Using the empirical relation between SFR and $L_{\rm H\alpha}$ (Kennicutt 1998), the 3 σ upper limit to the current SFR is 0.1 $M_\odot$ yr^{-1}.

A morphological fit to WIYN I-band imaging using galfit (Peng et al. 2002) shows good agreement with a de Vaucouleurs profile (Sérsic index = 4), with a χ^2/dof = 1.22. The effective radius is $R_e = 0″96 = 3.47$ kpc. The galaxy has an axis ratio of 0.81, with the semimajor axis aligned along a position angle east of north at ~90°. There was little improvement in χ^2/dof by adding more complicated morphologies or letting the Sérsic index vary.

The coincidence of a point source at radio wavelengths with the optical center of G1 might suggest the presence of a low-level active galactic nucleus, despite the lack of telltale features observed in the G1 optical spectra. Moreover, inspection of archival images of this galaxy from the Near-Earth Asteroid Tracking Program (Pravdo et al. 1999) on 2002 April 9, April 20, May 3, March 22, and April 8 reveals no apparent variability of the optical light from G1. However, radio emission without corresponding optical emission is not uncommon in giant elliptical galaxies harboring mildly active nuclei (Ho 1999). The radio emission in G1 is unlikely to be associated with star formation, given the low SFR deduced above.

The properties of this probable host galaxy contrast significantly with those measured for the galaxy hosts of long-duration GRBs. First, most hosts of long-duration GRBs exhibit emission-line features indicative of high SFRs (e.g., Djorgovski et al. 2003). Second, the absolute K-band luminosity of this galaxy ($\approx 1.6 \times 10^{11}$ $L_\odot$) exceeds that of all previously identified GRB host galaxies (Chary et al. 2002). Third, the impact parameter of the GRB (as defined by the 90% XRT error circle) is larger than that of all previously associated GRB-host galaxy pairs (long-burst offsets ≲10 kpc; Bloom et al. 2002).

5.1. S1, S2: Faint Blue Galaxies in a High-Redshift Group?

The Gemini GMOS spectra of S1 and S2 are featureless and blue. Examining the regions of the spectrum where $H\alpha$ or $H\beta$ would lie if at the redshift of the cluster, we detect no measurable emission. Assuming for the moment that the sources are at the cluster redshift of 0.22, we put a 3 σ upper limit on the $H\alpha$ luminosity of $L_{H\alpha} < 1.5 \times 10^{39}$ ergs s^{-1} and $L_{H\alpha} < 1.4 \times 10^{39}$ ergs s^{-1} for S1 and S2, respectively. Using the equation from Kennicutt (1998) relating the $H\alpha$ luminosity to the SFR, we find that the upper limits for the unextinguished SFR, assuming that S1 and S2 are cluster members, are $\sim 1.1 \times 10^{-2}$ $M_{\odot}$ yr^{-1} for the galaxies. If S1 and S2 are cluster members, then they are not forming stars, which would seem to conflict with their blue colors.

A more likely scenario, also mentioned by Cenko et al. (2005b), is that S1 and S2 are both background galaxies. Although the Gemini spectra range from 4600 to 8600 Å, the data have a poor signal-to-noise ratio blueward of 5200 Å. Nevertheless, the spectral slope is well constrained, and it suggests that these galaxies are forming stars (i.e., the continuum is relatively blue). The lack of corresponding emission lines ($H\alpha$, $H\beta$, [O III] $\lambda 5007$, and [O II] $\lambda 3727$) falling in our spectral window therefore suggests that S1 and S2 have $z \gtrsim 1.3$. Additional spectroscopy will be required to confirm our hypothesis that S1 and S2 are faint blue galaxy members of a small group at moderate redshift.

6. THEORETICAL INTERPRETATION

The fluence of the prompt gamma-ray emission measured by the *Swift* BAT is $f = (2.3 \pm 0.9) \times 10^{-8}$ ergs cm^{-2} (Barthelmy et al. 2005), which at the redshift of the tentative host implies an isotropic equivalent energy output of $E_{\gamma,iso} = (2.7 \pm 1) \times 10^{48}$ ergs. Since νF_ν is still rising roughly as $\nu^{0.5}$ in the 15–150 keV *Swift* range, the total fluence could be $\gtrsim 3$ times larger if the peak energy $E_p \gtrsim 1$–2 MeV. Figure 7 shows the isotropic equivalent luminosity of GRB X-ray afterglows scaled to $t = 10$ hr after the burst (in the cosmological rest frame of the source), $L_X(10\ \text{hr})$, as a function of their isotropic gamma-ray energy release, $E_{\gamma,iso}$, for GRB 050509b together with a sample of long GRBs. $L_X(10\ \text{hr})$ for GRB 050509b is estimated by extrapolating the flux measured by the *Swift* XRT using the best-fit power-law decay index of $\alpha = 1.3$, which is also consistent with the *Chandra* upper limit.

A linear relation, $L_X(10\ \text{hr}) \propto E_{\gamma,iso}$, seems to be broadly consistent with the data, probably suggesting a roughly universal efficiency for converting kinetic energy into gamma rays in the prompt emission for both short and long GRBs. This "universal" efficiency is also likely to be high (i.e., the remaining kinetic energy is comparable to, or even smaller than, that which was dissipated and radiated in the prompt emission). If this is the case, the well-known efficiency problem for long GRBs also persists for short GRBs.

The X-ray luminosity at 10 hr is used as an approximate estimator for the energy in the afterglow shock, since (1) at 10 hr the X-ray band is typically above both ν_m and ν_c so that the flux has a very weak dependence on ϵ_B [to the power of $(p - 2)/4$] and no dependence on the external density, both of which have relatively large uncertainties (Freedman & Waxman 2001; Piran et al. 2001; Berger et al. 2003); and (2) at 10 hr the Lorentz factor of the afterglow shock is sufficiently small ($\Gamma \approx 10$) so that a large fraction of the jet is visible (out to an angle of $\sim \Gamma^{-1} \approx 0.1$ rad around the line of sight) and local inhomogeneities on small angular scales are averaged out. Furthermore, the fact that the ratio of $L_X(10\ \text{hr})$ and $E_{\gamma,iso}$ is fairly constant for most GRBs suggests that both can serve as reasonable measures of the isotropic equivalent energy content of the ejected outflow. A possible
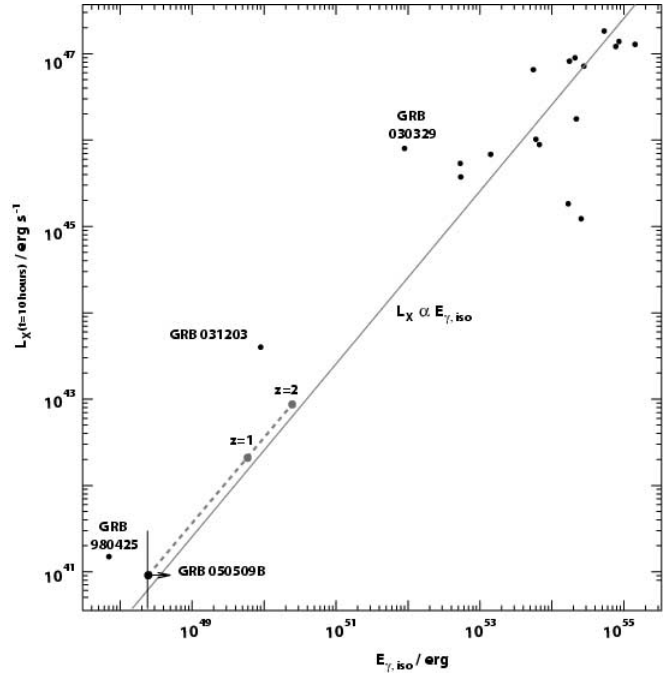

Fig. 7.—Isotropic equivalent luminosity of GRB X-ray afterglows scaled to $t = 10$ hr (source frame) after the burst, as a function of their isotropic gamma-ray energy release (adapted from Kouveliotou et al. 2004). If GRB 050509b is located at $z = 0.2248$, the isotropic equivalent luminosity of the X-ray transient at $t = 10$ hr, assuming $t^{-1.3}$, and the isotropic gamma-ray energy would be $\sim 9 \times 10^{40}$ ergs s^{-1} and $\sim 2.7 \times 10^{48}$ ergs, respectively (*large filled circle*).

caveat to the above statement arises if the observer is in fact not within the aperture of the GRB jet (as is suggested to be the case in both X-ray flashes and X-ray–rich GRBs; Granot et al. 2005). In this case $E_{\gamma,iso}$ can be significantly smaller than the isotropic equivalent kinetic energy in the afterglow shock, which is better reflected by $L_X(10\ \text{hr})$. This is likely to be the reason why GRB 031203 is above the correlation shown in Figure 7 (Ramirez-Ruiz et al. 2005). An off-axis interpretation for GRB 050509b, on the other hand, is unlikely, since its X-ray afterglow light curve was observed to decay from a very early epoch (at $t \approx 10^2$ s). This is also consistent with the fact that GRB 050509b falls close to the correlation.

The above arguments suggest that the energy in the outflow ejected by GRB 050509b was $\sim E_{\gamma,iso} \approx 10^{48.5}$ ergs, if it was spherical. On the other hand, if it was collimated into a narrow jet of half-opening angle θ_0, then the true energy would be smaller by a factor of $f_b = (1 - \cos \theta_0) \approx \theta_0^2/2$. Since a significant off-axis viewing angle is not likely, the true energy probably does not exceed $E_{\gamma,iso}$. A higher redshift would increase $E_{\gamma,iso}$ and with it the estimate for the energy release in this event; however, it would still remain significantly less energetic than typical long GRBs (see Fig. 7).

As also argued by Lee et al. (2005), the fact that the X-ray afterglow luminosity of GRB 050509b is much smaller than that of long GRBs is probably because the event was subenergetic rather than due to differences in the values of the external density or the microphysical parameters. This is illustrated in Figure 8 by a fit to the currently available afterglow data, using parameter values that are typical for long GRBs, except for the isotropic equivalent energy in the afterglow shock, $E_{k,iso}$, which is here taken to be equal to $E_{\gamma,iso}$ assuming $z = 0.2248$. Other parameter values could also give a reasonable description of the rather sparse data. In Table 3 we demonstrate a few different sets of parameters that fit the afterglow
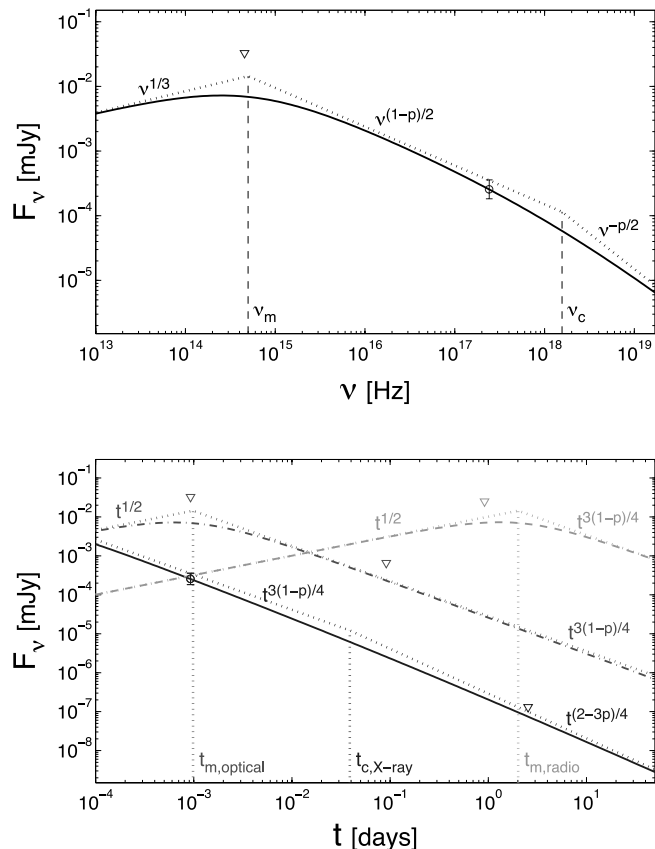
TABLE 3
REPRESENTATIVE FITS TO THE AFTERGLOW OF GRB 050509b

z	$E_{k,\mathrm{iso}}$ (ergs)	n (cm^{-3})	ϵ_e	ϵ_B	p	$E_{k,\mathrm{iso}}/E_{\gamma,\mathrm{iso}}$
0.2248......	2.75×10^{48}	1	0.15	0.046	2.2	1
0.2248......	1×10^{51}	1×10^{-6}	0.1	0.016	2.3	363
3..............	4.5×10^{50}	1	0.1	0.01	2.2	0.98
3..............	5.63×10^{52}	1×10^{-6}	0.1	0.01	2.3	122

NOTES.—An example of four different sets of parameters that fit the rather sparse afterglow data for GRB 050509b. In the first two cases we fix the redshift at that of the putative host galaxy (G1; $z = 0.2248$) and assume an external density that is either typical of the ISM, 1 cm^{-3}, or typical of the IGM, 10^{-6} cm^{-3}. In the last two cases we explore the option of a relatively high redshift, $z = 3$, with the same two very different values for the external density. In all cases, the values of the microphysical parameters (p, ϵ_e, and ϵ_B) were chosen to be typical of those inferred from afterglow fits for long GRBs.

FIG. 8.—Spectrum at $t = 80$ s after the trigger (*top*) and the light curves (*bottom*) of the X-ray (1 keV; *solid line*), optical (*R* band; *dot-dashed line*), and radio (4.9 GHz; *dashed line*) emission for a spherical afterglow shock propagating into a uniform ambient medium, using the model of Granot & Sari (2002). We also show the flux normalization in the X-rays from the *Swift* XRT detection, as well as upper limits in the optical and in the radio. Here we adopt the redshift of the tentative host galaxy ($z = 0.2248$) with *typical* interstellar medium density $n = 1$ cm^{-3} and assume that the isotropic equivalent kinetic energy in the afterglow shock is equal to $E_{\gamma,\mathrm{iso}}$ (i.e., 2.7×10^{48} ergs). The microphysical parameters are taken to be typical of those inferred from the modeling of afterglows of long GRBs: $p = 2.2$, $\epsilon_e = 0.15$, and $\epsilon_B = 0.046$. Table 3 gives other models consistent with the data. [*See the electronic edition of the Journal for a color version of this figure.*]

data. Again, we refer the reader to Lee et al. (2005) for a more detailed description. Regardless of the redshift, it will be very difficult to detect the afterglow in the radio, since the maximal flux density (given the observational constraints) is unlikely to exceed ∼15 μJy.

If short GRBs occur significantly outside of their host galaxies, as may be common for binary mergers (Tutukov & Yungelson 1994; Bloom et al. 1999; Fryer et al. 1999; Bulik et al. 1999; Belczyński et al. 2000), then one might expect the external density encountered by the afterglow shock of some GRBs to be very low, typical of the intergalactic medium (IGM), $n_{\mathrm{IGM}} \approx 10^{-6.5}(1 + z)^3$ cm^{-3}. This may help explain why some short bursts could have very faint afterglows. Since GRB 050509b happened to occur near the center of a galaxy cluster, where the external density is relatively high, its X-ray afterglow was relatively brighter. If indeed GRB 050509b is associated with the galaxy cluster at $z \approx 0.22$, then one might expect the external density to be intermediate between the IGM and ISM: the GRB is ∼76″ from the center of the cluster as determined by the X-ray position (§ 3.4), corresponding to ∼270 kpc in projection and well within the diffuse emission from the hot intracluster medium gas (which extends to a radius of ∼1 Mpc). This suggests

an ambient density near the position of the GRB of $n \approx 10^{-3}$ to 10^{-2} cm^{-3}, although this estimate is uncertain because the space position of the burst relative to the cluster center and the intracluster medium (ICM) density profile are not known precisely.

7. DISCUSSION

The lack of a strong afterglow signature sets GRB 050509b apart from most other GRBs.[25] As a comparison, the low-redshift long-soft burst (GRB 030329, $z = 0.1685$; Greiner et al. 2003), if placed at the redshift of G1, would have been $R \approx 14$ mag at $t = 8000$ s; this is approximately 10 mag brighter than the detection limits found here. Even at $z = 3$, the optical afterglow of a GRB 030329–like burst should have been detected at early times (neglecting the effects of dust extinction). Our non-detections ($R \gtrsim 24$ mag) of variability at 1.3 hr in what would be the rest frame at $z = 1$ is more than 3.5 mag deeper than the faintest optical transient found for a long GRB (GRB 021211, $z = 1.0$; see Fig. 2 of Fox et al. 2003).

The lack of detectable optical/infrared afterglow is not surprising considering, at face value, the putative progenitors and existing GRB afterglow theory. First, since the luminosity of long-wavelength afterglows scales with the square root of the ambient density (Begelman et al. 1993; Mészáros et al. 1998), events that occur in the ISM or IGM should be intrinsically fainter (at optical/infrared wavelengths) than those occurring in the circumburst environments of collapsars (see Panaitescu et al. 2001). Second, based on $\langle V/V_{\mathrm{max}} \rangle$ studies, the isotropic-equivalent peak luminosity [$L_p(\gamma)$] of short bursts is similar to that of long bursts (Schmidt 2001), implying that the total energy output [$E_{\gamma,\mathrm{iso}} \approx L_p(\gamma)/\eta \times$ duration, with η as the conversion efficiency to gamma rays] is at least an order of magnitude smaller for short bursts. As argued by Panaitescu et al. (2001), since afterglow brightness scales with $E_{\gamma,\mathrm{iso}}(1 - \eta)$, short-burst afterglows would be systematically faint.

Now that there is a detected X-ray afterglow, we are in a position to directly test the faintness claim by inferring the gamma-ray energy release and X-ray afterglow luminosity (a proxy for the kinetic energy in the blast wave). From Figure 7 it is clear that this ratio for GRB 050509b is similar to that found in long-duration GRBs. This is a striking observational bridge to long-duration bursts and suggests a common physical mechanism for prompt and delayed (afterglow) emission for both long-duration

[25] We note that two other low-luminosity, low-redshift GRBs (980425 and 031203) had detectable X-ray afterglow emission but no optical afterglow. The only transient optical signatures for these bursts were apparent supernovae.
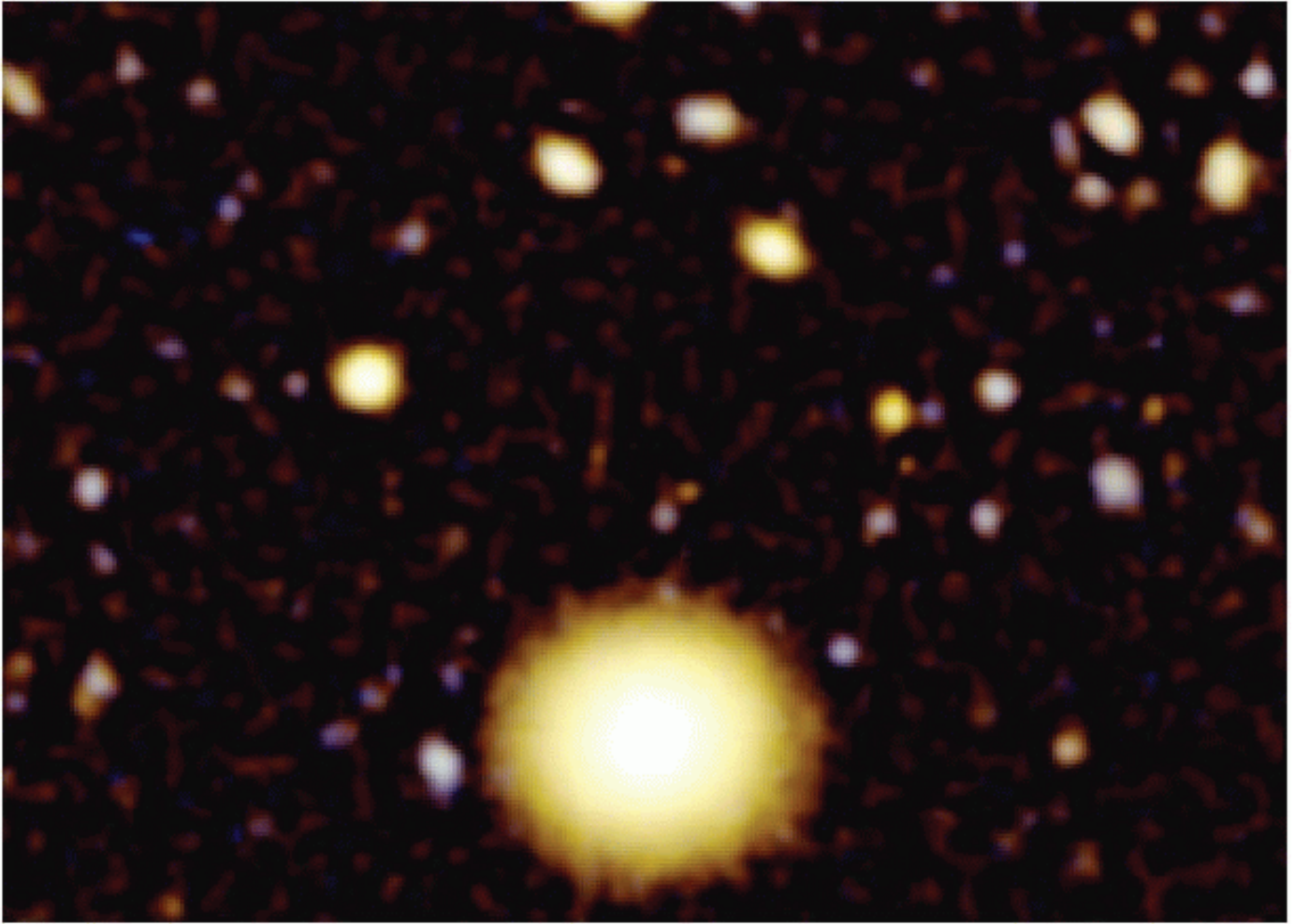
Fɪɢ. 9.—False-color image of the field of XRT constructed with the G (*blue*) and R (*red*) Keck LRIS images; green is interpolated between the observed bands. Aside from source S6 (which appears red) and possibly the J2/J4 complex, all of the XRT-consistent sources appear to be faint and blue, consistent with a small group of star-forming galaxies at a redshift larger than the cluster. As seen in this image, a number of such groups appear throughout the field (there are two faint blue galaxies to the north of G1, also embedded in the light of G1).

and short-duration GRBs, although their progenitors are probably different.

A tentative detection of an afterglow signal, achieved by adding up the emission of 76 short BATSE bursts, was reported by Lazzati et al. (2001; see also Connaughton 2002). The signal peaked at $t \approx 30$ s after the burst trigger, with a relatively flat $\nu F_\nu \approx 5 \times 10^{-10}$ ergs cm^{-2} s^{-1}. This would correspond to an X-ray flux in the 0.2–10 keV range of $F_X \approx 2 \times 10^{-9}$ ergs cm^{-2} s^{-1}. The X-ray flux of the afterglow of GRB 050509b is best constrained around $t \approx 200$ s and is found to be $F_X \approx 6.5 \times 10^{-13}$ ergs cm^{-2} s^{-1}. Extrapolating this flux to $t \approx 30$ s with a power-law index in the range inferred from the data, $1.0 \lesssim \alpha \lesssim 1.7$, gives a flux that is lower than the one found by Lazzati et al. (2001) by a factor of $\sim(1–5) \times 10^2$. This might suggest that either the possible detection by Lazzati et al. (2001) was not statistically significant or the X-ray afterglow of GRB 050509b is underluminous compared to the average value for short GRBs by at least 2 orders of magnitude.

With essentially no indication of recent star formation in G1, massive progenitor stars leading to collapsars cannot be present in G1. S1 and S2, the brightest and third-brightest sources within the XRT error circle, have no indication of recent star formation if their redshifts are $\lesssim 1.3$ (SFR < 0.05 $M_\odot$ yr^{-1} for $z < 0.3$, and SFR < 1 $M_\odot$ yr^{-1} for $z < 1.2$). The fainter (and blue) objects

discussed in § 5.1 are likely to be background galaxies. There are a number of blue galaxies in the field at comparable magnitude levels (Fig. 9). If the origin of GRB 050509b is from a collapsar, it is likely that its redshift exceeds 1.3.

If GRB 050509b is a background object at $z \gtrsim 2$, some progenitor scenarios are difficult to reconcile. With an observed duration of $\sim$30 ms, the rest-frame duration would only be about 10 ms. This is implausibly short for an NS-NS merger, and marginally possible for a BH-NS merger if the coalescence is through unstable mass transfer (Lee & Kluźniak 1999; Rosswog 2005; Miller 2005). It is hard to simultaneously accommodate the short intrinsic timescale and the higher energy budget of the burst within any compact merger model, if it is at high redshift.

If short GRBs trace star formation with a time delay through double compact mergers with coalescence timescales of 10^7–10^{10} yr (as opposed to prompt tracers of star formation, as with the collapsar scenario for long GRBs; Bagot et al. 1998; Bloom et al. 1999), then we expect some fraction (10%–30%) of short GRBs to be seen in association with early-type galaxies in general and clusters specifically (see Nutzman et al. [2004] for rate density in the local universe). This is somewhat model-dependent, since the distribution of compact merger timescales is poorly constrained by data but broadly consistent with both observed and model distributions.

A core-collapse supernova (SN) produces no electromagnetic radiation until its envelope is completely consumed by the explosion (although see Khokhlov et al. 1999). This phase ends, however, with a brilliant flash of X-ray or extreme ultraviolet photons as the shock reaches the stellar surface. The "breakout" flash is delayed in time, and vastly reduced in energy, relative to the neutrino transient produced by core collapse. However, it conveys useful information about the explosion. Shock breakout flashes were predicted by Colgate (1968) as a source for (the then-undetected) gamma-ray bursts. The explosion of SN 1987A stimulated a reanalysis of SN breakout flashes by Ensman & Burrows (1992) and, more recently, by Blinnikov et al. (1998, 2000). These studies represent an increase in sophistication toward the full numerical treatment of this complicated, radiation-hydrodynamic problem. In principle, the XRT data could constrain the existence of a shock breakout produced by both a red supergiant explosion like SN 1993J (Van Dyk et al. 2002) and a blue supergiant explosion analog to SN 1987A, but the X-ray luminosity is sensitive to the uncertain distribution of the extragalactic gas column and the specific XRT observing epochs.

Using our ESI optical imaging, we can also limit the presence of brightening due to a SN or SN-like emission at 8.17 days after the GRB to $R_C \approx 25.0$ mag. A normal, unextinguished Type Ia (thermonuclear) SN at $z = 0.22$ would have $R \approx 22$ mag around 6.7 days after explosion ($t = 8.17$ days in the observer's frame). A very subluminous SN Ia like SN 1991bg (Filippenko et al. 1992) would have $R \approx 24$ mag, still somewhat brighter than our limit. Extinction would obviously make the SN fainter, but the Milky Way contribution is small ($A_V \approx 0.06$ mag; Schlegel et al. 1998), and the outskirts of an elliptical galaxy in a cluster should have essentially no dust. While some core-collapse supernovae could be as faint as (or fainter than) our limit, the presence of such a supernova in the outskirts of an elliptical galaxy would be truly extraordinary (see van den Bergh et al. 2005). Others have also reported no evidence for a SN at later times (Hjorth et al. 2005a; Bersier et al. 2005).

The location of this short burst (and future short bursts) provides a useful discriminant for distinguishing between different progenitor models of short bursts. Simplistically, we would expect evaporating black holes to occur near the center of deep potential wells (as discussed in the context of Galactic BHs; Cline et al. 1999); thus, the offset from G1 seems to disfavor this hypothesis. A giant flare from a magnetar would need to have an isotropic luminosity ($L_{\gamma,\mathrm{iso}}$) larger by a factor of $\sim 10^3$ and an $E_{\gamma,\mathrm{iso}}$ larger by a factor of $\sim 10^2$ compared to the initial spike of the 2004 December 27 giant flare from SGR 1806−20 (the difference in the factor between the two quantities arises since GRB 050509b lasted only ~ 30 ms, which is ~ 10 times shorter than the initial spike of the giant flare from SGR 1806-20). Bursts from magnetars might be expected from galaxies of a later type than G1, where neutron stars would be formed copiously: magnetic field decay would cut the active lifetime for megaflare activity after $\sim 10^4$ yr.

8. CONCLUSIONS

We have monitored the location of GRB 050509b at optical and infrared wavelengths from 8 minutes to 8 days after the trigger and found no indication of variability at the location of the fading X-ray source, the first solid X-ray detection of an afterglow of a short-hard burst. Near the location of this source we and others have found an apparent group of faint blue galaxies at redshifts $\gtrsim 1.3$. While it is indeed plausible that this short burst arose from a progenitor connected with those gal-

axies, we found—based on a positional argument—plausible evidence that the progenitor is likely associated with 2MASX J12361286+2858580, a bright elliptical galaxy at $z = 0.2248$. We have argued that the observations find natural explanation with a compact merger system progenitor. If so, then short-hard GRBs provide a bridge from electromagnetic to gravitational wave astronomy: indeed, had GRB 050509b occurred a factor of ~ 3 closer in luminosity distance, it might have produced a detectable chirp signal with the next-generation Laser Interferometer Gravitational-Wave Observatory (LIGO II).[26]

Brightening emission from most types of supernovae would have been seen in our imaging, so the lack of such emission appears inconsistent with the notion that short bursts are due to collapsars or variants thereof. Our afterglow modeling is also consistent with, but does not require, a circumburst medium having lower density than that inferred in long-duration GRBs; if true, this would suggest that the progenitor produces a GRB in an environment that is baryon-poor compared to that expected for collapsars. Moreover, we have seen no evidence for ongoing star formation in the putative host, so there are likely no remaining massive stars. Given the short active life of a neutron star having a high magnetic field, this also disfavors the magnetar hypothesis.

The nondetection of brightening emission may place limits on the presence of a thermal "minisupernova" from nonrelativistic ejecta of a compact merger system (Li & Paczyński 1998; Rosswog & Ramirez-Ruiz 2002). In this scenario, the small dense mass (m_{ej}) ejected during coalescence expands as it is heated by radioactivity of the decompressed ejecta. Using the scalings of Li & Paczyński (1998) and crudely assuming that 10% of the bolometric light at peak is radiated in the R band, the R-band brightness should peak at observer time $t \approx 1.2(m_{\mathrm{ej}}/0.01\ M_\odot)^{1/2}$ days after the burst, with absolute magnitude $M_R \approx -18.5 - 1.25 \log(m_{\mathrm{ej}}/0.01\ M_\odot)$ mag. Assuming that the GRB did indeed originate from the redshift $z = 0.2248$, from inspection of Figure 2, with nondetections at $M_R \approx -16$ mag at $t \approx 1$ days, we can very roughly exclude $m_{\mathrm{ej}} >$ few $\times 10^{-3}\ M_\odot$. Although the Li & Paczyński (1998) model was intended as a simplistic sketch of the phenomenon, this limit on m_{ej} is somewhat surprising given the amount of escaping nonrelativistic material expected in compact mergers (Rosswog & Ramirez-Ruiz 2002). Indeed, we consider this lack of a minisupernova as weak evidence against a $z = 0.22$ origin from a compact merger system. Still, these limits are subject to considerable uncertainty in a number of uncertain parameters of ejecta. For instance, if the velocity of the ejecta were to be $\sim 0.01c$ instead of $0.3c$ (as assumed by Li & Paczyński 1998), then the peak of the thermal emission would occur after about 1 month and would not have been detected with the current limits.

We conclude by emphasizing that in the NS-NS or BH-NS progenitor hypothesis for short-hard bursts, the host galaxies may be a range of Hubble types (e.g., Livio et al. 1998). Compact merger systems coalesce in appreciable rates from Myr to Gyr after a starburst (e.g., Fryer et al. 1999; Bloom et al. 1999). Obviously, the longer the time since the starburst, the larger the distance a binary system will travel before coalescence. A clear prediction from this model is that as more short bursts are localized, those associated with later-type galaxies of *a given mass* should be preferentially closer to the star formation centers of the host; that is, we expect a more concentrated distribution around a spiral galaxy with the same mass as an early type. On

---

[26] See http://www.ligo.caltech.edu/docs/G/G990111-00.pdf.

the other hand, dwarf star–forming hosts have shallow enough potentials that merger systems from these galaxies could coalesce at appreciable distances ($\gtrsim 100$ kpc) even shortly after starburst. As *Swift* localizes more short-hard bursts, we expect that the offset distribution around galaxies will further elucidate the progenitor question.

REFERENCES

Arnaud, K. A. 1996, in ASP Conf. Ser. 101, Astronomical Data Analysis Software and Systems V, ed. G. H. Jacoby & J. Barnes (San Francisco: ASP), 17
Bacon, D. J., Massey, R. J., Refregier, A. R., & Ellis, R. S. 2003, MNRAS, 344, 673
Bagot, P., Portegies Zwart, S. F., & Yungelson, L. R. 1998, A&A, 332, L57
Barthelmy, S., et al. 2005, GCN Circ. 3385, http://gcn.gsfc.nasa.gov/gcn3/3385.gcn3
Begelman, M. C., Mészáros, P., & Rees, M. J. 1993, MNRAS, 265, L13
Belczyński, K., Bulik, T., & Zbijewski, W. 2000, A&A, 355, 479
Belczyński, K., Kalogera, V., & Bulik, T. 2002, ApJ, 572, 407
Berger, E., Kulkarni, S. R., & Frail, D. A. 2003, ApJ, 590, 379
Bersier, D., Fruchter, A., Rhoads, J., Levan, A., & Tanvir, N. 2005, GCN Circ. 3521, http://gcn.gsfc.nasa.gov/gcn3/3521.gcn3
Bessell, M. S. 1999, PASP, 111, 1426
Bethe, H. A., & Brown, G. E. 1999, ApJ, 517, 318
Blake, C. H., et al. 2005, Nature, 435, 181
Blanton, M. R., et al. 2003a, AJ, 125, 2348
———. 2003b, ApJ, 594, 186
Blinnikov, S. I., Eastman, R., Bartunov, O. S., Popolitov, V. A., & Woosley, S. E. 1998, ApJ, 496, 454
Blinnikov, S. I., Lundqvist, P., Bartunov, O., Nomoto, K., & Iwamoto, K. 2000, ApJ, 532, 1132
Blinnikov, S. I., Novikov, I. D., Perevodchikova, T. V., & Polnarev, A. G. 1984, Soviet Astron. Lett., 10, 177
Bloom, J., Blake, C., Prochaska, J. X., Hennawi, J., Gladders, M., & Koester, B. 2005a, GCN Circ. 3386, http://gcn.gsfc.nasa.gov/gcn3/3386.gcn3
Bloom, J., Blake, C., Prochaska, J. X., Hennawi, J., Gladders, M., Koester, B., & Chen, H.-W. 2005b, GCN Circ. 3388, http://gcn.gsfc.nasa.gov/gcn3/3388.gcn3
Bloom, J. S., Kulkarni, S. R., & Djorgovski, S. G. 2002, AJ, 123, 1111
Bloom, J. S., Sigurdsson, S., & Pols, O. R. 1999, MNRAS, 305, 763
Bloom, J. S., et al. 2005c, GCN Circ. 3417, http://gcn.gsfc.nasa.gov/gcn3/3417.gcn3
Breeveld, A., et al. 2005, GCN Circ. 3397, http://gcn.gsfc.nasa.gov/gcn3/3397.gcn3
Briggs, M. S., et al. 1996, ApJ, 459, 40
Bulik, T., Belczyński, K., & Zbijewski, W. 1999, MNRAS, 309, 629
Burrows, D. N., et al. 2000, Proc. SPIE, 4140, 64
Cenko, S. B., Soifer, B. T., Bian, C., Desai, V., Kulkarni, S. R., Berger, E., Dey, A., & Jannuzi, B. T. 2005a, GCN Circ. 3391, http://gcn.gsfc.nasa.gov/gcn3/3391.gcn3
———. 2005b, GCN Circ. 3401, http://gcn.gsfc.nasa.gov/gcn3/3401.gcn3
———. 2005c, GCN Circ. 3409, http://gcn.gsfc.nasa.gov/gcn3/3409.gcn3
Chary, R., Becklin, E. E., & Armus, L. 2002, ApJ, 566, 229
Cline, D., Matthey, C., & Otwinowski, S. 1999, ApJ, 527, 827
Colgate, S. A. 1968, Canadian J. Phys., 46, 476
Connaughton, V. 2002, ApJ, 567, 1028
Dar, A. 2004, preprint (astro-ph/0405386)
de Ugarte Postigo, A. D., Castro-Tirado, A. J., Eigenbrod, A., Jelinek, M., Gorosabel, J., & Guziy, S. 2005, GCN Circ. 3384, http://gcn.gsfc.nasa.gov/gcn3/3384.gcn3
Dickey, J. M., & Lockman, F. J. 1990, ARA&A, 28, 215
Djorgovski, S. G., et al. 2003, Proc. SPIE, 4834, 238
Eichler, D., Livio, M., Piran, T., & Schramm, D. N. 1989, Nature, 340, 126
Eisenstein, D. J., Hogg, D. W., & Padmanabhan, N. 2005, GCN Circ. 3418, http://gcn.gsfc.nasa.gov/gcn3/3418.gcn3
Engelbracht, C. W., & Eisenstein, D. J. 2005, GCN Circ. 3420, http://gcn.gsfc.nasa.gov/gcn3/3420.gcn3
Ensman, L., & Burrows, A. 1992, ApJ, 393, 742
Faber, S. M., et al. 2003, Proc. SPIE, 4841, 1657
Fenimore, E. E., et al. 2004, GCN Circ. 2735, http://gcn.gsfc.nasa.gov/gcn3/2735.gcn3
Filippenko, A. V. 1982, PASP, 94, 715
Filippenko, A. V., et al. 1992, AJ, 104, 1543
Fox, D. W., et al. 2003, ApJ, 586, L5
Freedman, D. L., & Waxman, E. 2001, ApJ, 547, 922
Freeman, P. E., Kashyap, V., Rosner, R., & Lamb, D. Q. 2002, ApJS, 138, 185
Frei, Z., & Gunn, J. E. 1994, AJ, 108, 1476
Fruchter, A., & Hook, R. N. 1997, Proc. SPIE, 3164, 120
Fryer, C. L., Woosley, S. E., & Hartmann, D. H. 1999, ApJ, 526, 152
Gal, R. R., de Carvalho, R. R., Lopes, P. A. A., Djorgovski, S. G., Brunner, R. J., Mahabal, A., & Odewahn, S. C. 2003, AJ, 125, 2064

Gandolfi, G., et al. 2000, in AIP Conf. Proc. 526, Gamma-Ray Bursts: 5th Huntsville Symposium, ed. R. M. Kippen, R. S. Mallozzi, & G. J. Fishman (Melville: AIP), 23

Gehrels, N., et al. 2005, preprint (astro-ph/0505630)

Granot, J., Ramirez-Ruiz, E., & Perna, R. 2005, ApJ, 630, 1003

Granot, J., & Sari, R. 2002, ApJ, 568, 820

Greiner, J., et al. 2003, Nature, 426, 157

Grossman, S. A., & Nowak, M. A. 1994, ApJ, 435, 548

Hjorth, J., et al. 2005a, ApJ, 630, L117

———. 2005b, GCN Circ. 3410, http://gcn.gsfc.nasa.gov/gcn3/3410.gcn3

Ho, L. C. 1999, ApJ, 510, 631

Hook, I. M., Jørgensen, I., Allington-Smith, J. R., Davies, R. L., Metcalfe, N., Murowinski, R. G., & Crampton, D. 2004, PASP, 116, 425

Horne, K. 1986, PASP, 98, 609

Huang, K. Y., et al. 2005, ApJ, 628, L93

Hurkett, C., et al. 2005, GCN Circ. 3381, http://gcn.gsfc.nasa.gov/gcn3/3381.gcn3

Hurley, K., Hartmann, D., Kouveliotou, C., Fishman, G., Laros, J., Cline, T., & Boer, M. 1997, ApJ, 479, L113

Hurley, K., et al. 2002, ApJ, 567, 447

———. 2005a, Nature, 434, 1098

———. 2005b, ApJS, 156, 217

Janka, H.-T., & Ruffert, M. 2002, in ASP Conf. Proc. 263, Stellar Collisions, Mergers and Their Consequences, ed. M. M. Shara (San Francisco: ASP), 333

Katz, J. I., & Canel, L. M. 1996, ApJ, 471, 915

Kehoe, R., et al. 2001, ApJ, 554, L159

Kelson, D. D., Illingworth, G. D., van Dokkum, P. G., & Franx, M. 2000, ApJ, 531, 159

Kennea, J. A., et al. 2005, GCN Circ. 3383, http://gcn.gsfc.nasa.gov/gcn3/3383.gcn3

Kennicutt, R. C. 1998, ARA&A, 36, 189

Khokhlov, A. M., Höflich, P. A., Oran, E. S., Wheeler, J. C., Wang, L., & Chtchelkanova, A. Y. 1999, ApJ, 524, L107

Kluzniak, W., & Lee, W. H. 1998, ApJ, 494, L53

Kouveliotou, C., Meegan, C. A., Fishman, G. J., Bhat, N. P., Briggs, M. S., Koshut, T. M., Paciesas, W. S., & Pendleton, G. N. 1993, ApJ, 413, L101

Kouveliotou, C., et al. 2004, ApJ, 608, 872

Lattimer, J. M., & Schramm, D. N. 1976, ApJ, 210, 549

Lazzati, D., Ghirlanda, G., & Ghisellini, G. 2005, MNRAS, 362, L8

Lazzati, D., Ramirez-Ruiz, E., & Ghisellini, G. 2001, A&A, 379, L39

Lee, W. H., & Kluźniak, W. Ł. 1999, MNRAS, 308, 780

Lee, W. H., Ramirez-Ruiz, E., & Granot, J. 2005, ApJ, 630, L165

Lee, W. H., Ramirez-Ruiz, E., & Page, D. 2004, ApJ, 608, L5

Le Floc'h, E., et al. 2003, A&A, 400, 499

Li, L.-X., & Paczyński, B. 1998, ApJ, 507, L59

Livio, M., et al. 1998, in AIP Conf. Proc. 428, Gamma-Ray Bursts: 4th Huntsville Symposium, ed. C. A. Meegan, R. Preece, & T. Koshut (Woodbury: AIP), 483

MacFadyen, A. I., & Woosley, S. E. 1999, ApJ, 524, 262

Matheson, T., et al. 2000, AJ, 120, 1487

Mazets, E. P., et al. 1981, Ap&SS, 80, 3

McHardy, I. M., et al. 2003, MNRAS, 342, 802

Mereghetti, S., Götz, D., von Kienlin, A., Rau, A., Lichti, G., Weidenspointner, G., & Jean, P. 2005, ApJ, 624, L105

Mészáros, P., Rees, M. J., & Wijers, R. A. M. J. 1998, ApJ, 499, 301

Miller, M. C. 2005, ApJ, 626, L41

Misra, K., & Pandey, S. B. 2005, GCN Circ. 3396, http://gcn.gsfc.nasa.gov/gcn3/3396.gcn3

Mochkovitch, R., Hernanz, M., Isern, J., & Martin, X. 1993, Nature, 361, 236

Mushotzky, R. F., & Loewenstein, M. 1997, ApJ, 481, L63

Nakar, E., Gal-Yam, A., Piran, T., & Fox, D. B. 2006, preprint (astro-ph/0502148)

Narayan, R., Paczyński, B., & Piran, T. 1992, ApJ, 395, L83

Norris, J. P., Cline, T. L., Desai, U. D., & Teegarden, B. J. 1984, Nature, 308, 434

Nutzman, P., Kalogera, V., Finn, L. S., Hendrickson, C., & Belczynski, K. 2004, ApJ, 612, 364

Oke, J. B., et al. 1995, PASP, 107, 375

Paczyński, B. 1986, ApJ, 308, L43

———. 1991, Acta Astron., 41, 257

Palmer, D. M., et al. 2005, Nature, 434, 1107

Panaitescu, A., Kumar, P., & Narayan, R. 2001, ApJ, 561, L171

Panchenko, I. E., Lipunov, V. M., Postnov, K. A., & Prokhorov, M. E. 1999, A&AS, 138, 517

Patel, S., Kouveliotou, C., Burrows, D. N., Grupe, D., Gehrels, N., Meszaros, P., Zhang, B., & Wijers, R. 2005, GCN Circ. 3419, http://gcn.gsfc.nasa.gov/gcn3/3419.gcn3

Peng, C. Y., Ho, L. C., Impey, C. D., & Rix, H. 2002, AJ, 124, 266

Pier, J. R., Munn, J. A., Hindsley, R. B., Hennessy, G. S., Kent, S. M., Lupton, R. H., & Ivezić, Ž. 2003, AJ, 125, 1559

Piran, T., Kumar, P., Panaitescu, A., & Piro, L. 2001, ApJ, 560, L167

Popham, R., Woosley, S. E., & Fryer, C. 1999, ApJ, 518, 356

Pravdo, S. H., et al. 1999, AJ, 117, 1616

Prochaska, J. X., Bloom, J., & Chen, H.-W. 2005a, GCN Circ. 3399, http://gcn.gsfc.nasa.gov/gcn3/3399.gcn3

Prochaska, J. X., Cooper, M., Newman, J., Bloom, J. S., Hurley, K., Blake, C., Gerke, B., & Chen, H. W. 2005b, GCN Circ. 3390, http://gcn.gsfc.nasa.gov/gcn3/3390.gcn3

Ramirez-Ruiz, E., Granot, J., Kouveliotou, C., Woosley, S. E., Patel, S. K., & Mazzali, P. A. 2005, ApJ, 625, L91

Rol, E., Page, K., Burrows, D. N., Gehrels, N., Goad, M., Hurkett, C., Kennea, J., & O'Brien, P. 2005, GCN Circ. 3395, http://gcn.gsfc.nasa.gov/gcn3/3395.gcn3

Rosswog, S. 2005, preprint (astro-ph/0504368)

Rosswog, S., & Ramirez-Ruiz, E. 2002, MNRAS, 336, L7

Rosswog, S., Ramirez-Ruiz, E., & Davies, M. B. 2003, MNRAS, 345, 1077

Rosswog, S., Speith, R., & Wynn, G. A. 2004, MNRAS, 351, 1121

Ruffert, M., & Janka, H.-T. 1999, A&A, 344, 573

Rykoff, E. S., Swan, H., Schaefer, B., & Quimby, R. 2005, GCN Circ. 3382, http://gcn.gsfc.nasa.gov/gcn3/3382.gcn3

Sasaki, M., Manago, N., Noda, K., & Asaoka, Y. 2005, GCN Circ. 3421, http://gcn.gsfc.nasa.gov/gcn3/3421.gcn3

Saz Parkinson, P. S. 2005, GCN Circ. 3411, http://gcn.gsfc.nasa.gov/gcn3/3411.gcn3

Schlegel, D. J., Finkbeiner, D. P., & Davis, M. 1998, ApJ, 500, 525

Schmidt, M. 2001, ApJ, 559, L79

Sheinis, A. I., Bolte, M., Epps, H. W., Kibrick, R. I., Miller, J. S., Radovan, M. V., Bigelow, B. C., & Sutin, B. M. 2002, PASP, 114, 851

Sipior, M. S., & Sigurdsson, S. 2002, ApJ, 572, 962

Soderbergh, A., & Frail, D. A. 2005, GCN Circ. 3387, http://gcn.gsfc.nasa.gov/gcn3/3387.gcn3

Terasawa, T., et al. 2005, Nature, 434, 1110

Torii, K. 2005, GCN Circ. 3393, http://gcn.gsfc.nasa.gov/gcn3/3393.gcn3

Tueller, J., et al. 2005, GCN Circ. 3005, http://gcn.gsfc.nasa.gov/gcn3/3005.gcn3

Tutukov, A. V., & Yungelson, L. R. 1994, MNRAS, 268, 871

van den Bergh, S., Li, W., & Filippenko, A. V. 2005, PASP, 117, 773

van der Horst, A. J., Wiersema, K., & Wijers, R. A. M. J. 2005, GCN Circ. 3405, http://gcn.gsfc.nasa.gov/gcn3/3405.gcn3

Van Dyk, S. D., Garnavich, P. M., Filippenko, A. V., Höflich, P., Kirshner, R. P., Kurucz, R. L., & Challis, P. 2002, PASP, 114, 1322

Wade, R. A., & Horne, K. 1988, ApJ, 324, 411

Windhorst, R. A., et al. 1991, ApJ, 380, 362

Woosley, S. E. 1993, ApJ, 405, 273

———. 2001, in Gamma-Ray Bursts in the Afterglow Era (Berlin: Springer), 257

Wozniak, P., Vestrand, W. T., Wren, J., Evans, S., & White, R. 2005, GCN Circ. 3414, http://gcn.gsfc.nasa.gov/gcn3/3414.gcn3